

**Analysis of cadmium, copper and lead ions in wine by ASDPV  
with a lab-made graphite composite working electrode.**

**Elyes Boubaker**

Dissertation submitted to **Escola Superior Agrária de Bragança – Instituto Politécnico de Bragança** to obtain the Degree of Master in **Food Quality and Safety** under the scope of the double diploma with the **Université Libre de Tunis**.

Supervised by

**Prof. Luís Avelino Guimarães Dias (IPB)**  
**Prof. Leticia Estevinho (IPB)**  
**Prof. Yassin Mokaddem (ULB)**

Bragança, Portugal

July 2021



## **Acknowledgements**

It is with enormous pleasure that I thank my esteemed thesis supervisor Prof. Luís Guimarães Dias for his continuous support, education, and mind enlightenment. This work would not have been possible without his efforts, which bore fruits since the first lesson of Advanced Analytical Techniques until this work presentation.

I wish also to thank my supervisors, Prof. Leticia Estevinho, and Prof. Yassine Mokaddem, for their valuable aid, and facilitation of this work. My gratitude goes to Eng<sup>o</sup>. David João Teixeira Alves Cabral, for his contribution to the thesis results.

I am thankful to the reference Polytechnic Institute of Bragança, as well to the Portuguese Republic, for receiving me in the best conditions and providing me all the means to achieve a considerable milestone in my career.

Finally, I would like to express my sincere and deepest recognition to my family for providing me with unfailing support and continuous encouragement throughout my years of study.

This Master thesis is a gift to my father Abdeljaoued Boubaker, my mother Najet Ben Mahmoud, and my brother Fares Boubaker.

Elyes Boubaker.



## Index

<b>ABSTRACT .....</b>	<b>IX</b>
<b>RESUMO.....</b>	<b>X</b>
<b>1. HEAVY METALS IN WINE .....</b>	<b>1</b>
1.1. VINIFICATION TECHNOLOGY .....	1
1.2. FACTORS OF HEAVY METALS PRESENCE IN WINE .....	2
1.2.1. <i>Natural environmental sources</i> .....	2
1.2.2. <i>Anthropogenic sources</i> .....	2
1.3. CHANGES IN WINE'S PROPERTIES .....	4
1.3.1. <i>Physicochemical properties</i> .....	4
1.3.2. <i>Organoleptic properties</i> .....	5
1.4. WINE'S TOXICITY OF HEAVY METALS IN HUMANS .....	5
1.4.1 <i>Legal limits</i> .....	5
1.4.2 <i>Toxicity in human health</i> .....	6
1.5. METHODS FOR HEAVY METAL ANALYSIS IN WINE .....	7
1.5.1. <i>Atomic Absorption Spectrometry</i> .....	7
1.5.2 <i>Inductively Coupled Plasma Optical Emission Spectrometry</i> .....	8
1.5.3. <i>Chromatographic and Electrophoretic Methods</i> .....	8
1.6. METAL ANALYSIS BY VOLTAMMETRY .....	9
1.6.1. <i>Voltammetry</i> .....	10
1.6.2. <i>Stripping voltammetry</i> .....	13
1.6.3. <i>Working electrodes used in the heavy metals' analysis</i> .....	17
1.7. EXPERIMENTAL DESIGNS .....	18
1.7.1. <i>Full factorial design</i> .....	18
1.7.2. <i>Central composite design</i> .....	20
1.7.3 <i>Response surface methodology</i> .....	21
<b>2. MATERIAL AND METHODS .....</b>	<b>22</b>
2.1. REAGENTS AND SAMPLES .....	22
2.2. ELECTROCHEMICAL ANALYSIS .....	23
2.2.1. <i>Equipment, cell and electrodes</i> .....	23
2.2.2 <i>Redox solution</i> .....	24
2.2.3. <i>Metal solutions</i> .....	26
2.3. FLAME SPECTROPHOTOMETER ANALYSIS .....	28
2.3.1. <i>Equipment</i> .....	28
2.3.2. <i>Standard calibration solutions and sample solutions</i> .....	28
2.4. ELECTROTHERMAL SPECTROPHOTOMETER ANALYSIS .....	29
2.4.1. <i>Equipment</i> .....	29
2.4.2. <i>Standard calibration solutions and sample solutions</i> .....	30
2.5. STATISTICAL ANALYSIS .....	31
<b>3. RESULTS AND DISCUSSION .....</b>	<b>32</b>
3.1. REDOX SOLUTION.....	32
3.1.1. <i>Cyclic voltammetry</i> .....	32
3.1.2. <i>Differential pulse voltammetry</i> .....	36
3.2. HEAVY METALS ANALYSIS.....	41
3.2.1. <i>Flame spectrophotometric analysis</i> .....	41
3.2.2. <i>Electrothermal spectrophotometric analysis</i> .....	43
3.2.3. <i>Electrochemical analysis</i> .....	45
<b>CONCLUSIONS.....</b>	<b>52</b>
<b>REFERENCES .....</b>	<b>53</b>

## Index of tables

Table 1. Maximum acceptable limits for metal ions, according to OIV regulation (Source: OIV Code Sheet – Issue 2012/01; European Union Regulation, 1990). .....	6
Table 2. Relevant works in the determination of heavy metals in wine by voltammetric techniques. ....	16
Table 3. Working Electrodes ( <a href="https://chem.libretexts.org/@go/page/61543">https://chem.libretexts.org/@go/page/61543</a> ).....	17
Table 4. Description of the wine sample.....	22
Table 5. Parameters defined for CV and DPV analyzes.....	25
Table 6. Experimental CCD of CV assays.....	25
Table 7. Experimental CCD of DPV assays .....	26
Table 8. Standard calibration solutions of $K_3[Fe(CN)_6]$ .....	27
Table 9. Mixed solution of the 3 heavy metals accordingly to the full factorial design .....	28
Table 10. Graphite furnace heating program.....	30
Table 11. RSM final model from response $I_{cp}$ obtained from the cyclic voltammograms .....	35
Table 12. RSM final model from response $\Delta I_p$ obtained from the differential pulse voltammograms.....	38
Table 13. Cadmium, copper and lead calibration curves results .....	41
Table 14. Heavy metal concentrations in wine by FAAS analysis * .....	42
Table 15. Cadmium, copper and lead calibration curves results .....	43
Table 16. Heavy metal concentrations in wine by ETAAS analysis * .....	44
Table 17. Models with the main effects for each heavy metal calibration .....	46
Table 18. Calibration curve parameters obtained from the analysis of the three metals by ASDPV with 2 and 4 min of deposition * .....	48
Table 19. Heavy metal concentrations in wine by ASDPV analysis * .....	49

## Index of figures

Figure 1. Levels of wine's contamination from air in a case of vineyard planted close to high traffic-roads (Helmerts, 1996).....	3
Figure 2. Electrochemical analytical methods (Cornelis et al., 2003).....	10
Figure 3. (A) Potential wave form for differential pulse voltammetry. (B) A typical differential pulse voltammogram (Kurbanoglu et al., 2017).....	11
Figure 4. Schematic of the voltametric electrochemical cell (Bontidean et al., 1998).....	12
Figure 5. CV, SWV, and DPV expected voltammograms (Weng et al., 2019). ....	13
Figure 6. Step of Stripping voltammetry (a) excitation signal (b) response curve (Cornelis et al., 2003).....	15
Figure 7. A 3 <sup>3</sup> full factorial design (27 points).....	19
Figure 8. Three one-third fractions of the 3 <sup>3</sup> design .....	20
Figure 9. Central composite design for 3 design variables at 2 levels.....	20
Figure 10. Electrochemical cell used in this work .....	23
Figure 11. Flame Atomic absorption spectrophotometer PerkinElmer PinAAcle 900T.....	29
Figure 12. Graphite furnace chamber (left figure) and the graphite tube used (right figure) 30	
Figure 13. Cyclic voltammogram obtained for the redox solution with the lab-made graphite composite working electrode.....	32
Figure 14. All cyclic voltammograms from the applied CCD with 2 factors .....	33
Figure 15. Linear relation between $I_{pc}$ and $I_{pa}$ .....	34
Figure 16. CV-RSM model residuals' plots of: residuals vs fitted; normal Q-Q; standardize residuals vs fitted values; standardized residual vs leverage, including cook's distance limits.....	35
Figure 17. 3D surface plot of the $I_{cp}$ values (CV response) in function of the two factors scan rate and potential pulse.....	36
Figure 18. Differential pulse voltammogram obtained for the redox solution with the lab-made graphite composite working electrode.....	37
Figure 19. All differential pulse voltammograms from the applied CCD with 3 factors .....	37
Figure 20. DPV-RSM model residuals' plots of: residuals vs fitted; normal Q-Q; standardize residuals vs fitted values; standardized residual vs leverage, including cook's distance limits.....	39
Figure 21. 3D surface plot of the DPV response $\Delta I_p$ values in function of the two factors scan rate and potential pulse.....	39
Figure 22. Calibration curve with $K_3[Fe(CN)_6]$ solutions and with 0.5M $Na_2SO_4$ .....	40
Figure 23. Calibration curve for cadmium, copper and lead obtained using FAAS.....	42
Figure 24. Calibration curve for cadmium, copper and lead obtained using ETAAS.....	44
Figure 25. ASDPV voltammograms of three standard solutions of calibration obtained using: (A) 2 min of deposition and (B) 4 min of deposition .....	46
Figure 26. Calibration curve for cadmium, copper and lead obtained using ASDPV with 2 and 4 min of deposition .....	47
Figure 27. ASDPV voltammograms with 4 min of deposition of samples W1 and R4 .....	50

*Figure 28. Linear relation between wine's Cu<sup>2+</sup> concentrations obtained with ASDPV analysis with 4 min of deposition vs. 2 min of deposition .....50*

*Figure 29. Linear relation between wine's Cu<sup>2+</sup> concentrations obtained with ASDPV analysis with 4 min of deposition vs. ETAAS analysis .....51*

## **Abbreviations**

3D: Three Dimensional

ANOVA: Analysis of Variance

ASDPV: Anodic Stripping Differential Pulse Voltammetry

ASV: Anodic Stripping voltammetry

BC: Background Corrector

C18 SPE: C18 solid phase extraction (SPE)

CCD: Central Composite Design

CE: Counter Electrode

CV: Cyclic Voltammetry

CZE: Capillary Zone Electrophoresis

DPV: Differential Pulse Voltammetry

$E^0$ : Formal Potential

Epa: Anodic Peak Potential

Epc: Cathodic Peak Potential

Epulse: Pulse Potential

Estep: Step Potential

ETAAS: Electrothermal Atomic Absorption Spectrometry

FAAS: Flame Atomic Absorption Spectrometry

FFD: Full Factorial Design

IC: Ion Chromatography

ICPMS: Inductively Coupled Plasma Mass Spectrometry

ICPOES: Inductively Coupled Plasma Optical Emission Spectrometry

IGPs: Integrated Graphite Platforms

Ipa: Anodic Peak Current

Ipc: Cathodic Peak Current

IPPG: Ion Permeability Porous Glass

LD: Limit of Detection

LQ: Limit of Quantification

LSV: Linear Sweep Voltammetry

MAL: Maximum Acceptable Levels

MRL: Maximum Residue Levels

OIV: Office International de la Vigne et du Vin (an international research and regulation center based in France)

R: Correlation Coefficient

$R^2$ : Determination Coefficient

RE: Reference Electrode

RSD%: Percentage Relative Standard Deviation

RSE: Relative Standard Error

RSM: Response Surface Methodology

SWV: Square Wave Voltammetry

THGA: Transversely Heated Graphite Atomizer

WE: Working Electrode

$\Delta i_p$ : Peak Current difference

## ABSTRACT

The purpose of the current study was to quantify the concentrations of copper, cadmium, lead ions in wine using ASDPV with a lab-made graphite composite electrode. A first study involved analysis of a reversible redox solution of  $K_3[Fe(CN)_6]$  with response surface methodology in order to verify the CV dependency with scan rate and potential step, as well the DPV dependency with scan rate, potential pulse and potential step. For the DPV analysis, the conditions selected were 0.03 V/s for the scan rate, 0.01 V for the step potential, and 0.04 V for the pulse potential. With these experimental conditions, the DPV data from a full factorial design using two concentration levels of the three heavy metals allowed to verify the independence between the calibrations of each metal.

The analysis of 8 samples of Portuguese and Spanish wines by ETAAS allowed to verify that only copper levels were detected and quantified, obtaining  $Cu^{2+}$  concentrations varying between 0.011 and 0.535 mg/L. Considering the heavy metals trace levels, the ASDPV technique was selected, with the 4 min deposition step for standard calibration solution and sample solutions, which demanded an assisted digestion with  $HNO_3$  and  $H_2O_2$ . The ASDPV showed higher sensibility toward the copper (slope of  $22 \mu A.L.mg^{-1}$ ), than cadmium (slope of  $14.2 \mu A.L.mg^{-1}$ ) and lead (slope of  $13.5 \mu A.L.mg^{-1}$ ). Only copper levels were measured in wine samples by ASDPV, within the range of 0.09 to 0.55 mg/L, being 0.91 times lower than those obtained by ETAAS.

Overall, the cheap lab-made graphite composite working electrode allows to analyze simultaneously three heavy metals using the ASDPV technique. Its analytical performance allows considering its application in the voltammetric analysis of wines. However, there is space for improvement by optimizing the experimental procedure of solutions preparations for ASDPV analysis which will be addressed in future work.

**Keywords:** Wine; Heavy metals; Cyclic voltammetry; Differential pulse voltammetry; Anodic stripping; Atomic absorption spectrophotometry; Response surface methodology; Experimental design.

## RESUMO

O objetivo do presente estudo foi quantificar as concentrações dos íons cádmio, cobre e chumbo no vinho usando ASDPV com um eletrodo compósito de grafite feito em laboratório. Um primeiro estudo envolveu a análise de uma solução redox reversível de  $K_3[Fe(CN)_6]$  com metodologia de superfície de resposta a fim de verificar a dependência da voltametria cíclica com a velocidade de varrimento e potencial de impulso, bem como a dependência da voltametria de impulso diferencial (DPV) com a velocidade de varrimento, potencial de impulso e potencial de incremento. Para a análise DPV, as condições selecionadas foram 0,03 V/s para a velocidade de varrimento, 0,01 V para o potencial de passo e 0,04 V para o potencial de incremento. Com estas condições experimentais, os dados de DPV de um desenho fatorial completo, utilizando dois níveis de concentração para os três metais pesados, permitiram verificar a independência entre as calibrações de cada metal.

A análise de 8 amostras de vinhos Portugueses e Espanhóis pela ETAAS permitiu verificar que apenas foram detetados e quantificados os teores de cobre, obtendo concentrações de  $Cu^{2+}$  a variar entre 0,011 e 0,535 mg/L. Considerando os níveis vestigiais dos metais pesados, foi escolhida a técnica redissolução anódica (anodic stripping, AS) com DPV, com a etapa de deposição de 4 min para as soluções padrão de calibração e soluções de amostra, após sofrerem digestão assistida com  $HNO_3$  e  $H_2O_2$ . A ASDPV apresentou maior sensibilidade em relação ao cobre (declive de  $22 \mu A.L.mg^{-1}$ ), do que para o cádmio (declive de  $14,2 \mu A.L.mg^{-1}$ ) e chumbo (declive de  $13,5 \mu A.L.mg^{-1}$ ). Apenas os teores de cobre foram medidos nas amostras de vinho por ASDPV, na faixa de 0,09 a 0,55 mg / L, sendo 0,91 vezes inferior aos obtidos pelo ETAAS. No geral, o eletrodo de trabalho compósito de grafite feito em laboratório permite analisar simultaneamente três metais pesados usando a técnica ASDPV. O seu desempenho analítico permite considerar a sua aplicação na análise voltamétrica de vinhos. No entanto, há espaço para melhorias, otimizando o procedimento experimental de preparação de soluções para análise de ASDPV que será abordado em trabalhos futuros.

**Palavras-chave:** Vinho; Metais pesados; Voltametria cíclica; Voltametria de pulso diferencial; Decapagem anódica; Espectrofotometria de absorção atômica; Metodologia de superfície de resposta; Desenho experimental.

# **1. HEAVY METALS IN WINE**

Wine is an alcoholic beverage that resulted from total/partial alcoholic fermentation of natural sugars present in fresh grape juice (Ribereau-Gayon et al., 2006). Its chemical composition contains sugar, polyphenolic compounds, amino acids, ethanol, water, organic compounds and inorganic compounds, which also include heavy metals (Tariba, 2011). Wine is likely the oldest alcoholic fermented beverage and was referenced in the holy scriptures book and in different records from Asian nations. The wines are classified as natural and appetizer wines, with respectively alcoholic content of 9° to 14° and 15° to 21°. Each wine is unique due to grape cultivar, phase of fruit development and ripening, utilization of added substances to the must, chemical composition of the fresh juice, wine-making techniques and maturing of wine, the sugar and alcohol content (Amerine et al., 1972).

## **1.1. VINIFICATION TECHNOLOGY**

Vinification includes three classes of operations: before fermentation, during fermentation and after fermentation. In white wine production, the juice is separated from the skin, which is not the case of red wine. Also, in the case of white wine the operations of centrifugation and sedimentation are used to clarify the wine, and at that point, yeast is added to the clear juice to begin the fermentation. However, in red winemaking, the seeds of grapes, pulp, and skins are kept together during squashing and fermentation (all or part) to obtain the characteristic flavor and color. Yeast is added to the must in red winemaking.

The yeasts during the wine fermentation process converts the sugars in the juice such as glucose, fructose, and sucrose into ethanol and carbon dioxide. When fermentation is finished, its clarification is accomplished by centrifugation, filtration, and racking. After, wine is racked off the yeast remains in oak barrels, or generally, in stainless steel vessels. During the storage stage, the wine might be blended, fined, filtered, and cold stabilized. The wine goes through changes during the time of maturation (Ribereau-Gayon et al., 2006), which tend to improve the flavor and taste of wine. However, the wine's quality is very important to assure its commercialization, being its contamination with heavy metals an important issue, which will be addressed in the next section.

## **1.2. FACTORS OF HEAVY METALS PRESENCE IN WINE**

The winemaking process contributes to the contamination of wine by heavy metals as Ca, Cr, Cu, Fe, Mg, Ni, As and Zn, being its levels dependent on environmental and anthropogenic sources (González-Larraina et al., 1987).

### **1.2.1. Natural environmental sources**

Firstly, the environmental impact is explained by the region where the grapes are planted, its weather conditions, and specifically the soil type and its organic and chemical compositions which influence the direct intake of heavy metals by the plant via the help of its roots (Aceto et al., 2003). For example, iron content in wine is affected by the region and which soil the vines are planted, being gathered by the plant's roots (Galani-Nikolakaki et al., 2002).

### **1.2.2. Anthropogenic sources**

Secondly, the anthropogenic sources are defined by the pollution or/and wrong techniques applied through the wine's production process, or manufacturing (Kment et al., 2005).

Generally, pollution (polluted air, contaminated water, wastewater pollution, industries, etc) is a huge factor contributing to heavy metals presence, increasing its significance year by year. As an example, the study of Helmers (1996) showed the significant transfer and contamination by platinum (Pt) of a vineyard close to high-traffic road, resulting in a wine with a high concentration of Pt at final stage of production. The Figure 1 present a schematic of Pt contamination through the chain production of the wine, from the vine to grape, to wine (Helmers, 1996).

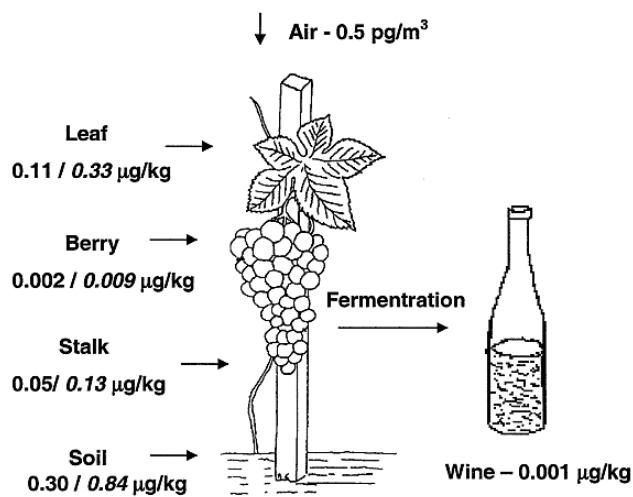


Figure 1. Platinum contamination levels in wine in a case of vineyard planted close to high traffic-roads (Helmerts, 1996).

Another main source of heavy metal contamination may occur during the wine's production process, like the phytosanitary treatments, chemical fertilizers and hormones that regulate the grape growth. These wrong agricultural techniques can cause contamination of the soil and irrigation water, contributing to a contaminated grape by heavy metals (Riganakos et al., 2003). For example, copper concentration levels have a correlated relation with the application of copper as a fungicide in the vineyard to treat mildew (Catarino et al., 2005); or, arsenic exceeded content in wine is caused by the intensive application of insecticide and herbicides (Ibanez et al., 2008). After grapes harvest, the winemaking process takes place having also a significant role in the contamination by heavy metals (Kment et al., 2005), like the long contact of wine with the containers (Riganakos et al., 2003). For example, the production process can cause an increment in zinc concentration in wine, as well as, the use of fertilizers containing zinc (Galani-Nikolakaki et al., 2002); some additives can trigger the accumulation of heavy metals in wine, like using Cu in order to delete undesirable odors through fermentation and wine maturation (Kristl et al., 2003; Tromp et al., 1988); the addition of bentonite, which is used to avoid tartaric acid precipitations to clarify wines, can contribute to the increment of aluminum presence in wine (Pennington et al., 1989); finally, the storage of wine in stainless-steel is a considerable factor to the contamination of wine by heavy metals, having the oak barrels less contribution (Lopez et al., 1998). With the aging of wine, this contribution increases, mainly the heavy metals such as chromium, due to the continuous contamination via stainless steel (Volpe et al., 2009).

Overall, the heavy metals contamination in wine (from the techniques and treatments applied all along the wine's production chain) is a big issue since they can contribute to changes in wine quality (González-Larraina et al., 1987).

### **1.3. CHANGES IN WINE'S PROPERTIES**

#### **1.3.1. Physicochemical properties**

The clarity of wine is one of the most important characteristics of wine, which is caused by particles in suspension in the form of flocculating or sediment. Metal ions, organic acids, and phenolic compounds are abundant in wine but, under certain conditions (including exposure to light, exposure to oxygen (O<sub>2</sub>), temperature, and other variable parameters), can cause a negative change in colour and undesirable taste (Ribereau-Gayon et al., 2006). However, the turbidity increases with the metal concentrations, especially above a certain threshold value. For instance, some heavy metals like Co, Al, Fe, Zn, and Ni, are responsible for turbidity formation throughout the wine fermentation and storage (Galani-Nikolakaki et al., 2002; Kment et al., 2005).

Vinification is a long process that involves a series of techniques and manipulations, where wine can come into contact with oxygen that reacts with certain compounds in the wine (Ribereau-Gayon et al., 2006). For instance, copper and iron are believed to be the main catalysts for the non-enzymatic oxidation of wine, even in low quantities. Although, the oxygen in its ground state cannot react with other organic molecules (Danilewicz, 2003), the hydrogen peroxide (H<sub>2</sub>O<sub>2</sub>), formed after oxygen reduction in the presence of ferric ions and its reaction with phenolic compounds in wine, is more reactive and can be reduced by either Fe<sup>+2</sup> or Cu<sup>+2</sup> ions in the absence of bisulfite (Kreitman et al., 2013). The formation of quinones, a result of the oxidation of phenolics that contain catechol or pyrogallol (non-enzymatic oxidation) can cause browning and loss of aromas (Laurie et al., 2012). Moreover, both the oxidation products of wine, H<sub>2</sub>O<sub>2</sub>, and quinones, can react with the main preservative used in the wine (sulfur dioxide, SO<sub>2</sub>) which results in a loss of it during the oxidation of the wine and, once it falls below a certain concentration, microbial deterioration and/or aromas and colour defects will occur in the wine (Barril et al., 2012). All these undesirable effects, due to the oxidation of wine, are frequently catalysed by heavy metals being the objective to maintain a low concentration of heavy metals in wine (Esparza et al., 2005). Moreover, a specific group of

aromas known as “reductive” are formed when the wine contains no oxygen during the winemaking process or when little oxygen is available again after bottling (Ugliano et al., 2011). These undesirable aromas are generally caused by the presence of hydrogen sulfide, methanethiol and dimethyl sulfide, which are by-products of alcohol fermentation (Viviers et al., 2014). The heavy metals such as Co and Fe can influence not only oxidation but also to this reducing process in wine if there are present in sufficient concentrations, through increases in the by-product’s concentration mentioned previously (Viviers et al., 2013). So, heavy metals can cause changes in wine characteristics, such as organoleptic and chemical properties, being important to identify the factors of their contamination (Aceto et al., 2003).

### **1.3.2. Organoleptic properties**

The alteration of organoleptic properties of wine, like unwanted modifications of taste, aroma, and colour can also be due to the high levels of heavy metals. They tend to form complexes with anthocyanins together with tannins and contributing to the occurrence of redox reactions, causing wine astringency, turbidity, browning during aging and cloudiness (Pohl, 2007; Pyrzynska et al., 2007; Li et al., 2008).

Moreover, heavy metals like Zn, Ni, Cu and Al play a part in haze-forming proteins accompanied with change of colour due to the complex’s formation with tannins and anthocyanins (Esparza et al., 2005). Also, high concentrations of CuO and Fe affect the wine quality, through oxidative alteration causing browning, iron taste, wine cloudiness and deterioration of aroma and taste (Cacho et al., 1995; Kment et al., 2005).

## **1.4. WINE’S TOXICITY OF HEAVY METALS IN HUMANS**

### **1.4.1 Legal limits**

Aside from the effect on wine quality, metals in wine may likewise affect negatively human health above certain limits which are often referred to as “Maximum Residue Levels” (MRL) or “Maximum Acceptable Levels” (MAL). Indeed, even moderate consumption of such wines can introduce danger to human health. Specifically, heavy metals can be complexed to phenol compounds in wine and so, at the acid gastric pH (1.5-3.5), they can be accessible for adsorption and can cause toxic effects (WHO, 1992). Table 1 presents MAL values in wine for

the most significant heavy metals, issued by the Office International de la Vigne et du Vin (OIV an international research and regulation center based in France).

*Table 1. Maximum acceptable limits for metal ions, according to OIV regulation (Source: OIV Code Sheet – Issue 2012/01; European Union Regulation, 1990).*

Element	Maximum Acceptable Limit (mg/L)
Lead (Pb)	0.15
Cadmium (Cr)	0.1
Zinc (Zn)	5.0
Arsenic (As)	0.2
Copper (Cu)	1.0

### **1.4.2 Toxicity in human health**

Essential metals as Fe, Zn and Cu are needed in a wide physiological function, however, if the recommended limit intake of heavy metals is exceeded, it may cause either acute or chronic toxic effects. For instance, light levels of Cu in wine can incite gastrointestinal side effects like diarrhea, vomiting, nausea, and abdominal and muscle pain, and can cause damage to the kidneys and liver (WHO, 1998). Actually, toxic heavy metals, like Al, As, Cd and Pb, have no known dietary benefit or physiologic function in the human body, and their concentration in wine should be kept as low as possible because of their expected harmful impacts. Aluminum has been related to the harmful of various neurodegenerative problems, for example, Parkinson's disease and Alzheimer's disease (Solfrizzi et al., 2006). Berthon (2002) explained that organic acids present in high concentrations in wine can expand the ingestion of Al in the gastrointestinal tract just like a cancer-causing agent to both humans and animals, being a possible cause of the skin, lung, and bladder cancers. According to Pyrzyńska (2004), an overabundance of ingested Pb may lead to damage in nervous system and biosynthesis of hemoglobin. Even low degrees of Pb intake are connected with hypertension, cardiovascular illness, kidney disfunction, impaired sperm production and osteoporosis (WHO, 1977; Telisman et al., 2001; Telisman et al., 2007). Also, Cd is very toxic even at low concentrations and may lead to bioaccumulation, principally in the liver and kidneys (WHO, 1992).

Considering that wine consumption doesn't cause a high intake of heavy metals, its moderate consumption may come with health benefits and contribute to the well-being of the cardiovascular system. However, the consumption of wine with excessive concentration of

heavy metals can cause risk to human health, especially for those who drink over 250 ml of such wine daily over a lifetime (Naughton et al., 2008).

## **1.5. METHODS FOR HEAVY METAL ANALYSIS IN WINE**

In order to control or monitor the heavy metals concentrations during the different steps of vinification mentioned earlier, analytical methods are used. Among many methods for metal determination, atomic/emission/mass spectrometry, ion chromatography, capillary zone electrophoresis and also electrochemical methods have been used. The majority of heavy metals can be determined with these techniques at concentrations ranging from mg/L to µg/L levels (Angelova et al., 1999).

### **1.5.1. Atomic Absorption Spectrometry**

The official methods for the determination of metals in wine recommended by the OIV and the American Society of Enologists are essentially based on flame atomic absorption spectrometry (FAAS) due to its selectivity, high sensitivity, and capability for direct measurements. Alkali metals and alkali earth metals as well as many of the transition metals like Mn, Cu, Fe or Zn are all atomized with good efficiency using a common air/acetylene flame with typical detection limits in the sub-ppm range (Sauvage et al., 2002). Usually, precision analysis is 2%. The high concentration of potassium in wines (generally 300–1500 mg/L) acts as a natural ionization buffer. This is a critical factor for alkaline metals determination because it causes a decrease in their ionization and a corresponding increase in the signal. Moreover, in the presence of high concentration of phosphate (300–800 mg/L of  $\text{PO}_4^{2-}$ ), the metals Ba, Ca, Mg, Sr, and Al should be analyzed in the presence of a releasing agent (normally LiCl) (Aceto et al., 2002), since it allows to avoid their refractory phosphate compounds. Electrothermal atomic absorption spectrometry (ETAAS) is mainly used for trace metals determination in wine samples (Lopez et al., 1998). However, during the direct analysis of complex matrixes, the nonspecific background absorption from interfering chemical species often occurs and could cause serious problems. For most of these elements, a Beer's law relationship will hold between approximately 0.5 and 15–20 ppm, which means that FAAS will not be able to determine the concentration of an analyte that is below or above this range (Freschi et al. 2001). As an example, the study conducted by Bora et al., (2015) showed that by applying FAAS method to

quantify the heavy metals present in wine, it was possible to detect a contamination of the wine obtained from the Fetească Regală variety by zinc at a concentration ( $5.69 \pm 0.46$  mg/L) which exceeded the maximum admitted limit (5 mg/L) (Bora et al., 2015).

### **1.5.2 Inductively Coupled Plasma Optical Emission Spectrometry**

Inductively Coupled Plasma Optical Emission Spectrometry (ICPOES) can be used to perform multielement determination in wine, but the detection limit for most metals is in the range of 1 to 10  $\mu\text{g/L}$ . This method has considerably wide dynamic range, making it a more suitable technique for highly concentrated samples or samples with wide concentrations of the analyte. ICP-OES accuracy proved to depend on wine composition, since it showed severe positive interferences from inorganic cations, especially calcium and potassium, and negative interferences from glucose and ethanol, the major organic components of wine (Zerbinati et al., 2000). Although these interferences are opposite in sign, there is little probability that they can compensate each other due to the large variability of wine composition. Two of the strengths of the Inductively Coupled Plasma Mass Spectrometry (ICPMS) technique are its multielement capability and the low detection limits obtained for most elements.

These techniques can be an important tool for comparison of elemental compositions of different wines, for instance, for sample's origin. But despite many advantages of these techniques, one of the main problems is the high consumption of plasma-forming gas, which make it costly to perform the analysis (Castineira et al., 2001). As an example, a study conducted by Voica et al. (2009) in an attempt to characterize Romanian wines from the point of view of their heavy metal content, 13 samples representing different wine assortments were analyzed using ICPOES. Thirty metals were identified including heavy metals with concentrations ranging from 0.02  $\mu\text{g/L}$  to 6 mg/L. High toxicity heavy metals like Pb, Cd and As showed concentrations barely below the limits imposed by OIV (Voica et al., 2009).

### **1.5.3. Chromatographic and Electrophoretic Methods**

Ion chromatography (IC) with conductivity detection, which is commonly used for determining alkaline and alkaline earth metals in different types of samples, was also applied for quantification of these cations in wine (Zerbinati et al., 2000). This method has less interferences than ICPOES since the analyte peaks are separated quite well. The accuracy of

IC determination conditions was less sensitive to wine composition than to instrumental conditions, which can be effectively controlled. However, a preliminary clean-up procedure with C18 solid phase extraction (SPE) cartridges had to be adopted to separate matrix components responsible for long stabilization times. Capillary zone electrophoresis (CZE), as an alternative technique to IC, can be readily applied to the analysis of both cations and anions. The content of some metals (Na, K, Ca, Mg, Mn and Li) in a variety of red wines produced in different geographical zones of Galicia (northwestern Spain) was determined in a single run by CZE. Samples were injected using hydrostatic injection for 30 s and indirect UV detection at 214 nm was applied. The developed method showed good precision for the migration time of the analytes (0.09–0.209% RSD) and for the peak area (2.5–3.4% RSD) (Halicz et al., 1996). These previously mentioned techniques, which allows to quantify heavy metals in wine, are sensitive and selective, but they require relatively expensive instruments, application of complex operational procedures and demands long detection times (Siraj et al., 2013). The electrochemical techniques are alternative due to their simplicity, high sensitivity, low cost, speed, portability, and appropriateness for monitoring of direct monitoring in the field.

## **1.6. METAL ANALYSIS BY VOLTAMMETRY**

Electrochemical analytical techniques can be divided into two main groups (Cornelis et al., 2003): analysis occurs in the interface between solution and electrode's surface (electrodics); analysis takes place in the solution bulk (ionics).

Figure 2 presents the main electrochemical analytical techniques that differ by the signal measured and electrical parameter controlled, giving different physics, and chemical information, for instance, rate constants for chemical reaction, quantitative analysis, and number of electrons involved in redox reactions, etc (Bertrand, 1997). As can be seen, the most electroanalytical techniques are affiliated to the group of electrodics (Cornelis et al., 2003).

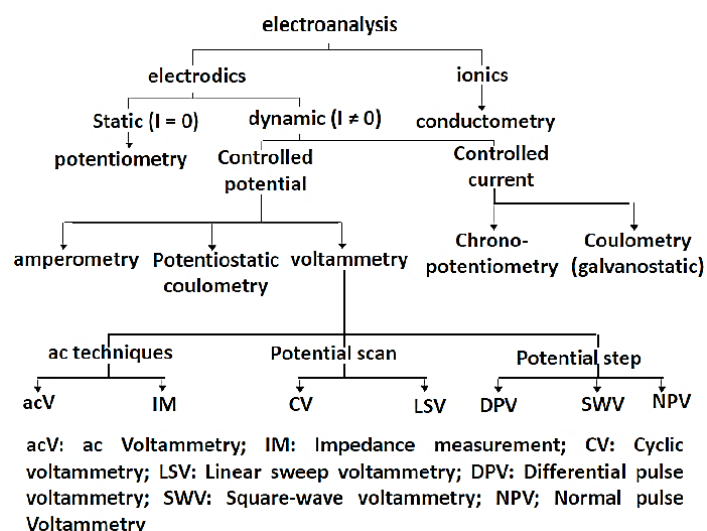


Figure 2. Electrochemical analytical methods (Cornelis et al., 2003).

### 1.6.1. Voltammetry

For quantitative analysis, the electrochemical technique that has great sensitivity and can be applied for *in situ* detection of heavy metals contamination is voltammetry. Voltammetry has shown great developments, mainly with the appearance of new working electrodes either through the use of different materials or through the modification of working electrode surfaces, which allows for more comprehensive analytical applications. The carbon working electrodes is one of great interest over the metal electrodes because of their comparatively low cost, high chemical stability and wide range of potential window (Yang et al., 2016). The voltammetric techniques are considered active techniques because they apply potential that causes a change in the concentration of electroactive molecules on the electrode's surface by redox reaction (reactions that depends on potential, current, and time). As an example, Figure 3 presents the typical potential scan in time (first plot) for the differential pulse voltammetry technique and the expected signal, current values, in relation to the applied potential (Bertrand, 1997; Gunzler et al., 2001).

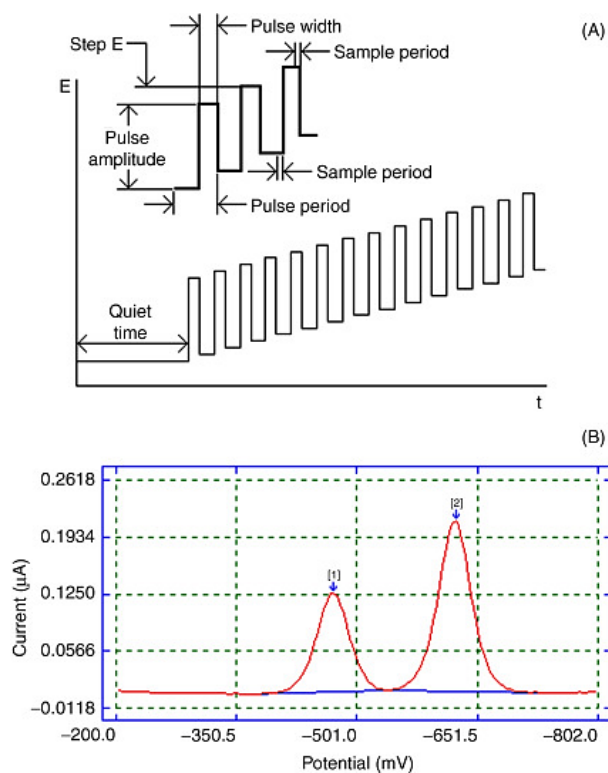


Figure 3. (A) Potential wave form for differential pulse voltammetry. (B) A typical differential pulse voltammogram (Kurbanoglu et al., 2017).

Usually, an analytical electrochemistry system has three parts: an electrolyte, an electrochemical cell composed of three electrodes (WE-working electrode, CE-counter electrode and RE-reference electrode) and a potentiostat equipment (Bontidean et al., 1998). Figure 4 presents a schematic of a typical electrochemical cell for voltammetry analysis, with three electrodes configuration (letter A is the orientation direction of response current flow during reduction and letter B, the orientation direction of electrons flows during oxidation) (Bontidean et al., 1998).

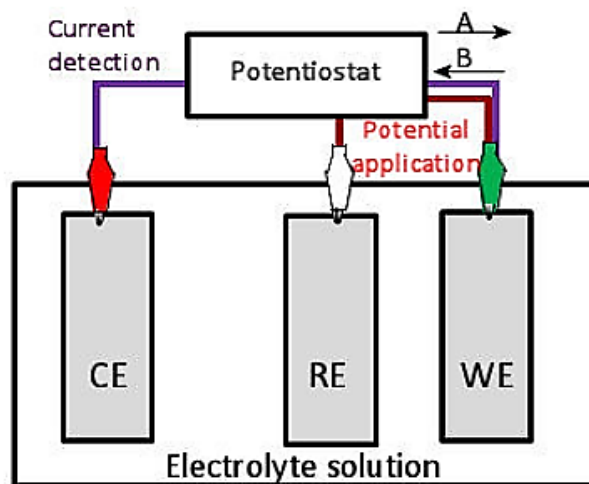


Figure 4. Schematic of the voltammetric electrochemical cell (Bontidean et al., 1998). WE- working electrode; RE- reference electrode; CE- counter electrode.

In voltammetry, the current signal is created by two different currents:

- faradic current, related to the flux from the analyte reduction or oxidation, which magnitude is related to the concentrations of the analytes in solution and all kinetic operations happening on the electrode, it based on Faraday's law (Gunzler et al., 2001);
- capacitive current, produced by the interface electrode-solution without a relation with the process of electron transfer, resulting mostly only in background signals in the measurement analytical.

Capacitive current should be isolated from the faradic current or make it insignificant for quantitative analysis. Applying micro-electrodes and using techniques of step potential such as pulse techniques (as, square wave voltammetry, SWV, and differential pulse voltammetry, DPV) allow to eliminate the capacitive current (Gunzler et al., 2001).

The most used voltammetry techniques are DPV and SWV, as potential step methods (Figure 5), as well as, linear sweep voltammetry (LSV) and cyclic voltammetry (CV), as potential scan methods. The best voltammetry techniques, in terms of sensitivity, for heavy metals detection are SWV and DPV (Silva et al., 2014), which also allows the simultaneous analysis of several heavy metals. As an example of applications, Wang et al., (2012) have reported the quantification of lead with an excellent linear range from 5 to 2000  $\mu\text{g/L}$  with a detection limit of 1  $\mu\text{g/L}$ , using a gold microelectrode. Also, a study by Saturno et al. (2011) reported the electroanalytical determination of heavy metals utilizing DPV equipped with a glassy carbon working electrode, by achieving a limit of detection of 18  $\mu\text{g/L}$  and 11  $\mu\text{g/L}$ , respectively for

lead and cadmium. Figure 5 show CV, SWV and DPV expected voltammograms (Weng et al., 2019).

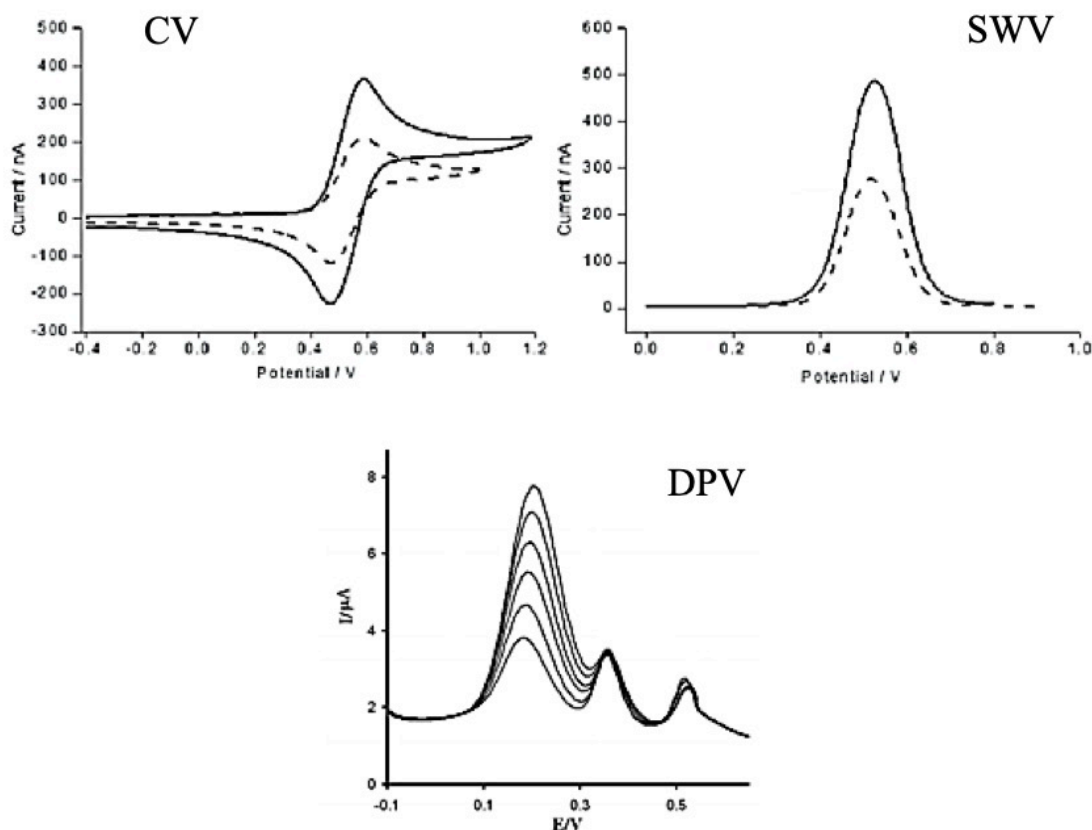


Figure 5. CV, SWV, and DPV expected voltammograms (Weng et al., 2019). CV- cyclic voltammetry; SWV- square wave voltammetry; DPV- differential pulse voltammetry.

However, for the analysis of trace concentrations of heavy metals, stripping voltammetry is usually applied since it is an electrochemical technique that allows to pre-concentrate the heavy metals levels in the electrode's surface, before analysis.

### 1.6.2. Stripping voltammetry

The stripping techniques permits a lower detection limit than other electrochemical methods, demanding a simple sample's preparation and allowing good selectivity and sensitivity (Bertrand, 1997; Hernandez, 2006; Gunzler et al., 2001). This technique comprises of three primary steps: pre-concentration, resting and stripping.

The pre-concentration step gives various modes to pre-concentration of the analyte on the working electrode surface, which can be done electrochemically (electrolysis) or by adsorption.

This step is carried out in large solution's volume and, the posterior analysis, in a volume much smaller. For reproducible results is important to control the hydrodynamic parameters as, pre-concentration time, stirring, temperature, electrode area, and the initial potential applied (Ambel, 1999). The pre-concentration permits to increase sensitivity in 2-3 orders of magnitude, allowing to analyze heavy metal concentrations of  $10^{-10}$  mol/L, or even lower (Ambel, 1999).

In the resting step, the electrolysis and stirring is stopped after a controlled period of time and has a period of resting during which the applied potential remains unchanged, thus ensuring that no re-oxidation of the metal by traces of oxygen takes place and, through this time, homogenization of metals on the surface of the working electrode is achieved together with recovering the diffusion regime (Ambel, 1999).

The stripping step occurs after the preconcentration step, the deposited heavy metals are oxidized ("stripped") from the working electrode back into the solution by oxidation to the ionic form under conditions of diffusion control (applying a potential sweep in the opposite direction to the initial). The anodic diffusion current is used to determine the concentration of the metals in the working electrode's surface, which is proportional to time of electrolysis, stirring rate and concentration of metals in solution. Figure 6 shows the stripping step, as well as, the voltammogram obtained from the analysis of three heavy metals using a mercury working electrode (Cornelis et al., 2003).

With this technique, the resulting heavy metals concentrations to be detected in the electrode is significantly greater than in the analyzed solution and is much smaller than the volume of the solution due to the volume of the electrode (Cornelis et al., 2003).

After stripping step is complete, the potential is changed using LSV, DPV or SWV, resulting in oxidation of a heavy metal, amalgam or alloy, returning to solution and recording a current peak due to this process. The height of the current peak is related to the heavy metal's detected concentration in the electrode which is proportional to the heavy metal's concentration present in the solution. Quantitative analysis is possible if analytical experimental parameters are kept constant such as, the area of the working electrode, pre-concentration time, time and potential of the heavy metal's deposition, stirring conditions, temperature, etc. For instance, the required deposition time depends on the analytes concentrations and can reach a value of  $10^{-9}$  mol/L in 20 minutes (Cornelis et al., 2003). However, the use of graphite electrodes in the electrochemical analysis presents an interesting alternative for eliminating mercury and decreasing the adverse effect of organic substances, besides its low cost, wide potential

window, relatively inert electrochemistry, and electrocatalytic activity for a variety of redox reactions (Brainina et al., 2000; Brainina et al., 1996).

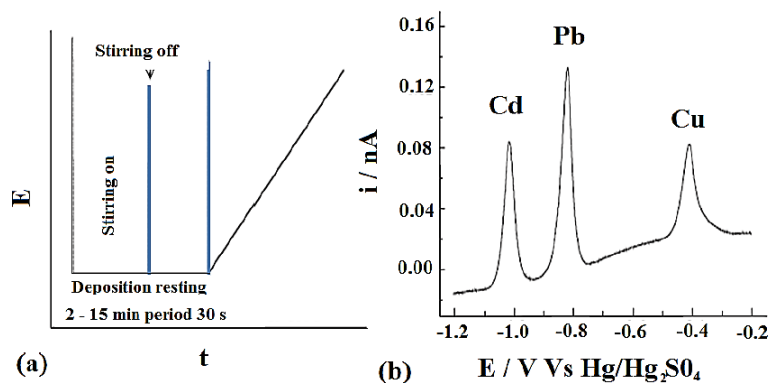


Figure 6. Step of stripping voltammetry (a) excitation signal (b) response curve (Cornelis et al., 2003).

As an example, a study conducted by Brainina et al. (2004) showed the potential of anodic stripping voltammetry (ASV) with the use of graphite-containing electrodes by performing the analysis of heavy metals in wine by ASV and comparing them with the standardized ICPMS method to confirm the voltammetric results. It revealed that the concentrations of copper, lead, cadmium and zinc ions in dry wines (contains 9–12% alcohol and less than 3 g/l sugar) determined by the proposed ASV method and the ICPMS method, are quite equivalent. Slightly higher differences were found for cadmium, but the measured concentrations were near the practical detection limit of the used procedure for ICPMS. However, good coefficient of determination ( $R^2$ ) of 0.999, 0.990, 0.978 and 0.988 were obtained for copper, lead, cadmium and zinc, respectively (Brainina et al., 2004).

Table 2 summarizes the information of several studies of heavy metals analysis in wine by electrochemical methods, presenting the technique used, the metals analyzed and the concentration levels obtained, as well the working electrodes applied.

Overall, the ASV method together with the DPV was the most used since, it allows to do a pre-concentration of the heavy metals. These studies showed results with precision, high speed of scan and the capability of voltammetry techniques to detect a wide range of heavy metals simultaneously in wine.

Table 2. Relevant works in the determination of heavy metals in wine by voltammetric techniques.

Heavy metals	Levels (mg/L)	Technique *	Working electrode applied	Reference
Cu Pb Zn	0.42 ± 0.05 0.15 ± 0.01 0.58 ± 0.05	ASV	Electrode with 0.1-mm electroconducting graphite containing layers applied onto two side walls of the electrolyzer	Stozhko et al., 2005
Zn Cd Pb Cu	0.0538 ± 0.00045 0.00369 ± 0.00029 0.0179 ± 0.00097 0.00195 ± 0.06	ASDPV	Hanging mercury drop electrode (HMDE)	Maciel et al., 2019
Cu Pb Cd Zn	0.519 ± 0.02 0.067 ± 0.007 0.00026 ± 0.00005 0.54 ± 0.047	ASV	Thick-film modified graphite-containing electrode (TFMGE)	Brainina et al., 2004
Cd Zn	0.002 0.148	ASDPV	Mercury microelectrode	Daniele et al., 1989
Zn Pb Cu	0.549 ± 0.02 0.115 ± 0.008 0.112 ± 0.008	ASDPV	Mercury electrode	Garrido et al., 1997
Pb Cu Cd	0.110 0.08 0.0019	ASDPV	Hanging mercury drop electrode	Oehme et al., 1979
Cu	0.56	ASDPV	Mercury electrode	Wiese et al., 1997
Zn Pb	0.3691 0.0567	ASDPV	Solid silver amalgam electrode	Mikkelsen et al., 2002

\*) ASDPV - anodic stripping differential pulse voltammetry; ASV - anodic stripping voltammetry.

### 1.6.3. Working electrodes used in the heavy metals' analysis

The WE represents the most important component of an electrochemical cell. It is at the interface between the WE and the solution that electron transfers of greatest interest occur. The selection of a working electrode material is critical to experimental success. Several important factors should be considered. Firstly, the material should exhibit favorable redox behavior with the analyte, ideally fast, reproducible electron transfer without electrode fouling. Secondly, the potential window over which the electrode performs in a given electrolyte solution should be as wide as possible to allow for the greatest degree of analyte characterization. Additional considerations include the cost of the material, its ability to be machined or formed into useful geometries, the ease of surface renewal following a measurement and toxicity. The Table 3 presents the advantages and disadvantages of the main types of working electrodes.

Table 3. Working Electrodes (<https://chem.libretexts.org/@go/page/61543>)

Material	Advantages	Disadvantages
Graphite	<ul style="list-style-type: none"><li>- Many types and configurations</li><li>- Good cathodic potential range</li><li>- Low cost</li></ul>	<ul style="list-style-type: none"><li>- Quality varies greatly</li><li>- Hard to shape</li></ul>
Platinum	<ul style="list-style-type: none"><li>- Good electrochemical inertness</li><li>- Large range of sizes</li></ul>	<ul style="list-style-type: none"><li>- Expensive</li><li>- Low hydrogen overvoltage so cathodic potential range limited</li></ul>
Gold	<ul style="list-style-type: none"><li>- Configurations same as Pt</li><li>- Larger cathodic potential range</li></ul>	<ul style="list-style-type: none"><li>- Larger cathodic potential range</li><li>- Anodic window limited by surface oxidation</li><li>- Expensive</li></ul>
Mercury	<ul style="list-style-type: none"><li>- Excellent cathodic window</li><li>- Easy to "refresh"</li><li>- Forms amalgams</li></ul>	<ul style="list-style-type: none"><li>- Limited anodic window due to mercury oxidation</li><li>- Toxic</li></ul>

#### 1.6.3.1. Graphite working electrode

Carbon-based materials such as graphite, carbon fibers, etc. have recently been used as the conductive phase in composite materials suitable for electrochemical sensors (Fei et al., 2007; Niwa, 2005). The use of composites based on a conductive material dispersed within an insulating polymer matrix as electrode has led to important advances in developing sensor

devices (Moghaddam et al., 2007; Zhu et al., 2007). The composite materials consisted of a combination of two or more materials, in which each individual component exhibits its original characteristic, with the distinctive chemical, mechanical and physical peculiarities. Electrodes obtained by using a mixture of particulate conductive carbon phase and an insulating matrix represent an attractive approach for the fabrication of electrochemical sensors, whose surfaces can be renewed by polishing (Ramírez-García et al., 2002; Rassaei et al., 2007).

## **1.7. EXPERIMENTAL DESIGNS**

The importance of, and theoretical concepts behind, experimental design and optimization methodology in research and development efforts has been thoroughly discussed in a number of informative publications (Myers, 1971; Otto, 1999). The two main applications of experimental design are screening, in which the factors that influence the experiment are identified, and optimization, in which the optimal settings or conditions for an experiment are found. The usual approach is to start with a screening design including all controllable factors that may possibly influence the experiment, identify the most important ones, and proceed with an experimental optimization design. Models generated can be evaluated by the analysis of variance (ANOVA). The one-way ANOVA allows experimenters to compare several groups of observations. A two-way ANOVA allows one to study the effects of two factors separately as well as their interactive effects (Hanrahan et al., 2005).

### **1.7.1. Full factorial design**

To obtain an approximation model that evaluates the interactions between  $N$  variables, a full factorial design (FFD) approach may be necessary to investigate all possible combinations (Montgomery, 1997), since in this kind of design, all variables are varied together, instead of one at a time. A  $2^N$  full factorial design has two levels under study (-1 and +1), being  $N$  the number of variables to study and, similarly, a  $3^N$  full factorial design studies the main and interaction effects with 3 levels (-1, 0 and +1), being  $N$  the number of variables to study.

As an example, a  $3^3$  full factorial design includes 3 levels (can represent 3 values of concentration, temperature, pH, etc) for each of the 3 variables under study that will allow to evaluate a response (result from analysis), A spatial representation of these assays is shown in Figure 7.

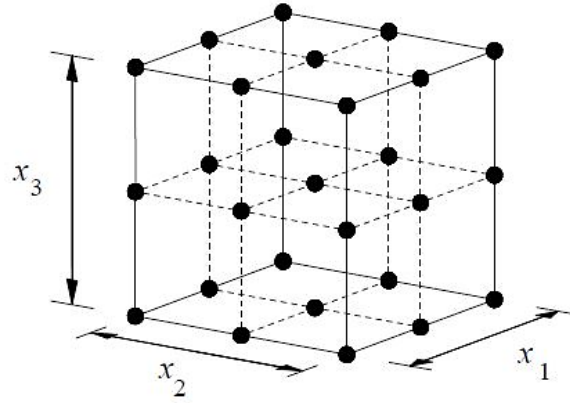


Figure 7. A  $3^3$  full factorial design (27 points)

Factorial designs can be used for fitting second-order models. A second-order model can significantly improve the optimization process when a first-order model suffers lack of fit due to interaction between variables and surface curvature. A general second-order model is defined as

$$y = a_0 + \sum_{i=1}^n a_i x_i + \sum_{i=1}^n a_{ii} x_i^2 + \sum_{i=1}^n \sum_{i=1}^n a_{ij} x_i x_j \quad ,$$

where  $x_i$  and  $x_j$  are the design variables and  $a_x$  are the tuning parameters.

The construction of a quadratic response surface model in  $N$  variables requires the study at three levels so that the tuning parameters can be estimated, being needed at least  $(N+1)(N+2)/2$  function evaluations. Generally, the number of experiments grows exponentially ( $3^N$  for a full factorial) with the number of variables, which can be impractical. A full factorial design typically is used for five or fewer variables and, if the number of design variables becomes large, a fraction of a full factorial design can be used at the cost of estimating only a few combinations between variables. This is called fractional factorial design and is usually used for screening important design variables.

For a  $3^N$  factorial design, a  $(\frac{1}{3})^p$  fraction can be constructed resulting in  $3^{N-p}$  assays. For example, for  $p=1$  in a  $3^3$  design, the result is a one-third fraction, often called  $3^{3-1}$  design, as shown in Figure 8 (Montgomery, 1997).

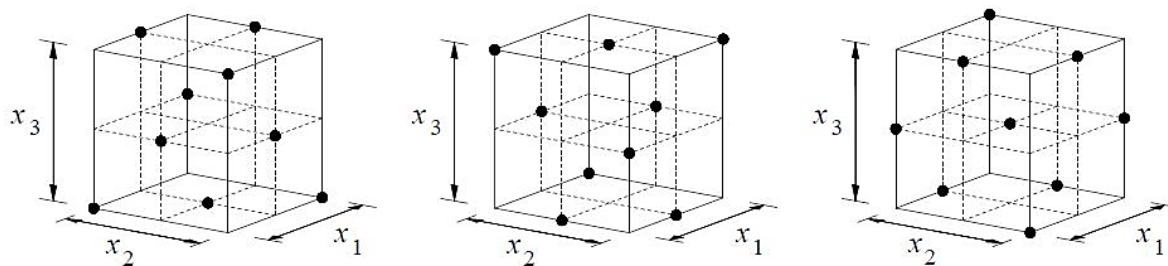


Figure 8. Three one-third fractions of the  $3^3$  design

### 1.7.2. Central composite design

The second-order model can be constructed efficiently with central composite designs (CCD) (Montgomery, 1997). CCD are first-order ( $2^N$ ) designs augmented by additional center and axial points to allow estimation of the tuning parameters of a second-order model. Figure 9 shows a CCD for  $3^3$  design variables, which allows the construction of second-order models because the number of experiments is reduced as compared to a full factorial design (15 in the case of CCD compared to 27 for a full-factorial design).

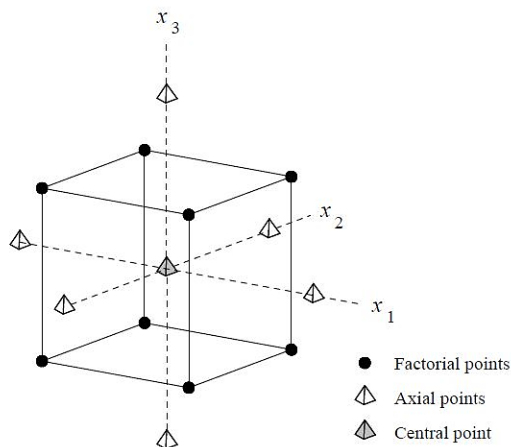


Figure 9. Central composite design for 3 design variables at 2 levels

As an example of CCD application on voltammetry, a central composite rotatable design was used to evaluate the effects of the variables using a gold nanoparticle modified carbon working electrode by the differential pulse voltammetry method to detect betaxolol in the presence of acetaminophen. These variables include scan rate, step potential, modulation amplitude, gold nanoparticles content and pH. The results indicated that the gold nanoparticle modified carbon paste electrode could be employed for the determination of betaxolol in real samples such as pharmaceutical formulations and plasma sample (Ghoreishi et al., 2012).

### **1.7.3 Response surface methodology**

Response surface methodology (RSM) consists of a group of mathematical and statistical techniques that are based on the fit of empirical models to the experimental data obtained using an experimental design (Bruns et al., 2006). This term was originated from the graphical perspective generated after fitness of the mathematical model, and its use has been widely adopted in texts on chemometrics. Linear or square polynomial functions are employed to describe the system studied and, consequently, to explore (modeling and displacing) experimental conditions until its optimization (Teofilo et al., 2006). The application of RSM as an optimization technique has several steps: (1) the selection of independent variables of major effects on the system through screening studies, (2) the delimitation of the experimental region, according to the objective of the study and the experience of the researcher; (3) the choice and application of the experimental design; (4) the mathematic–statistical treatment of the obtained experimental data through the fit of a polynomial function; (5) the evaluation of the model’s fitness; (6) the verification of the necessity and possibility of performing a displacement in direction to the optimal region; and (7), the definition of the optimum values for each studied variable.

## 2. MATERIAL AND METHODS

### 2.1. REAGENTS AND SAMPLES

The reagents used were:

- Potassium chloride, KCl, Panreac AppliChem (Spain)
- Sodium sulfate, Na<sub>2</sub>SO<sub>4</sub>, Panreac AppliChem (Spain)
- Sodium acetate, CH<sub>3</sub>COONa, Panreac AppliChem (Spain)
- Acetic acid, CH<sub>3</sub>COOH, Panreac AppliChem (Spain)
- Potassium ferricyanide, K<sub>3</sub>[Fe(CN)<sub>6</sub>], Panreac AppliChem (Spain)
- Nitric acid, HNO<sub>3</sub>, Panreac AppliChem (Spain)
- Hydrogen peroxide 30%, H<sub>2</sub>O<sub>2</sub>, Panreac AppliChem (Spain)
- Stock standard solution of cadmium (Cd<sup>2+</sup>), 1000 mg/L, Panreac AppliChem (Spain)
- Stock standard solution of copper (Cu<sup>2+</sup>), 1000 mg/L, Panreac AppliChem (Spain)
- Stock standard solution of lead (Pb<sup>2+</sup>), 1000 mg/L, Panreac AppliChem (Spain)

All solutions were prepared with deionized water (type II), obtained from an ATS deionization equipment containing a reverse osmosis system and a column with anionic and cationic resins. Eight wine samples were used in this work, collected in a commercial center, being their general description presented in Table 4.

*Table 4. Description of the wine sample*

<b>ID</b>	<b>Type</b>	<b>Geographic origin</b>	<b>Year</b>	<b>Alcohol %</b>
R1	Red wine	Badajos, Spain	2020	11
R2	Red wine	Trás-os-Montes, Portugal	2020	14
R3	Red wine	Alentejo, Portugal	2019	13.5
R4	Red wine	Alentejo, Portugal	2019	13.5
W1	White wine	Badajos, Spain	2020	11
W2	White wine	Badajos, Spain	2020	11
W3	White wine	Tejo, Portugal	2019	12.5
W4	White wine	Douro, Portugal	2020	12

## 2.2. ELECTROCHEMICAL ANALYSIS

Electrochemical analyses were carried out with a lab-made graphite composite working electrode, being this section about the description of the analytical system used and the working electrode performance tests, as well as, its application in the analysis of three heavy metals (cadmium, copper and lead ions) in wine.

### 2.2.1. Equipment, cell and electrodes

The potentiostat used was a portable Palmsens EmStat MUX8 (Netherlands), and the voltammograms were collected using the software PsTrace 5.2, developed by the same company. The voltammetric setup consisted in a custom-made electrochemical cell containing three electrodes (lab-made working electrode, the reference electrode, and the counter electrode), as described below (Figure 10).

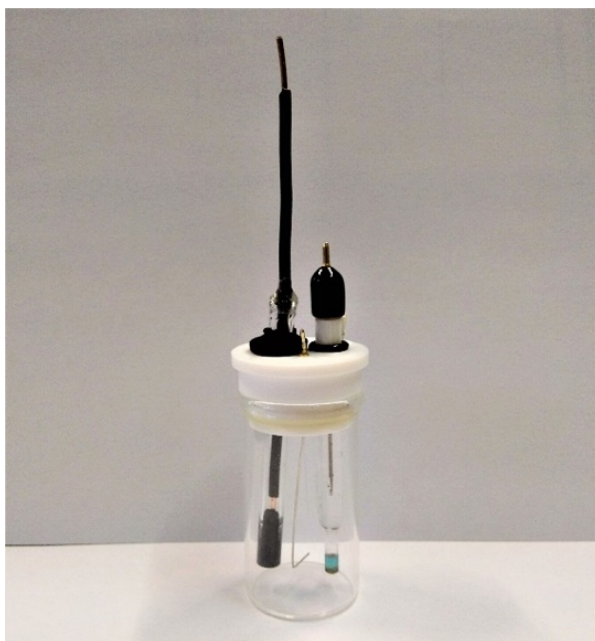


*Figure 10. Electrochemical cell used in this work*

The working electrode was constructed with a ratio of 50% of graphite, dried during 24 h at 105 °C in a Memmert UL 50 oven (Germany), and 50% of Crystal Araldite® from the Standard Syringe 24 ml ARA-4000030003 (United Kingdom), which is a neutral glue having an equal amount of resin and hardener. Then, the mix was incorporated into a thin glass tube with a

diameter of 0.5 mm, fixing the copper wire with a diameter of 3 mm in the cylinder's center point. After, it was dried at 40 °C in the oven, during overnight.

A silver chloride (Ag/AgCl) reference electrode was used, a 70 mm long and 3.5 mm of outer diameter glass tube filled with electrolyte solution (3.0 mol/L KCl, saturated with AgCl) and with an IPPG (Ion Permeability Porous Glass) tip at the lower end. An Ag wire coated with AgCl is connected via a 1.0 mm diameter pin at the top end of the electrode. This pin can accept an alligator clip.

The CE was a 6 cm long platinum wire with 0.5 mm diameter. It was attached to a Teflon cap. The upper side has a gold-plated pin which accept an alligator clip.

## **2.2.2 Redox solution**

The reversible reaction was evaluated using a aqueous redox solution constituted by 0.01M potassium ferricyanide ( $K_3[Fe(CN)_6]$ ; 329.24 g/mol; 0.329 g in 100 mL) and 0.5 M sodium sulfate ( $Na_2SO_4$ ; 142.04 g/mol; 7.10 g in 100 mL).

### ***2.2.2.1. Response surface methodology***

For the study of the WE, in CV it was verified the effects of the scan rate and pulse potential and in DPV, scan rate, step potential, and pulse potential. The experimental conditions used in voltammetric analysis for both techniques are presented in Table 5.

The purpose was to evaluate the influence of these parameters in order to reach the best response, as well to obtain voltammograms with low noise, reversible redox reaction, and round intense peaks, acceptable intensity and good baseline. Two CCDs were used, one with 2 factors (14 assays with 2 blocks) for the CV assays (Table 6) and another, with 3 factors (20 assays with 2 blocks) for DPV (Table 7). Table 5 presents the levels -1 and +1 (range of parameters) of the factors studied and which were applied to the CCDs shown in Tables 6 and 7. Each assay was carried out using the same redox solution (described previously), using 10 mL of the redox solution plus 0.1 mL of KCl 3M, and 0.1 mL of acetate buffer (mixture of acetic acid 0.10 mol/L with  $CH_3COONa$  0.10 mol/L until pH 4.65 is obtained with a pH electrode).

Table 5. Parameters defined for CV and DPV analyzes

Parameter	CV
Initial Potential, V	-0.40
Initial Potential Time, s	5
Sweep Potential 1, V	-0.40
Sweep Potential 2, V	0.92
Sweep Potential 3, V	-0.40
Number of cycles	5
Scan, V/s	Level -1 = 0.029; Level +1 = 0.17
Potential step, V	Level -1 = 0.0058; Level +1 = 0.34

Parameter	DPV
Initial Potential, V	-1.0
Initial Potential Time, s	5
Final Potential, V	1.0
Time pulse, s	0.01
Number of cycles	5
Scan, V/s	Level -1 = 0.10; Level +1 = 0.049
Potential step, V	Level -1 = 0.00047; Level +1 = 0.0075
Potential pulse, V	Level -1 = 0.0038; Level +1 = 0.076

Table 6. Experimental CCD of CV assays

Assay order	Scan rate, V/s	Potential step, V	Block
1	0.100	0.020	1
2	0.150	0.030	1
3	0.050	0.010	1
4	0.100	0.020	1
5	0.150	0.010	1
6	0.050	0.030	1
7	0.100	0.020	1
8	0.100	0.0058	2
9	0.100	0.034	2
10	0.171	0.020	2
11	0.10	0.020	2
12	0.100	0.020	2
13	0.029	0.020	2
14	0.100	0.020	2

Table 7. Experimental CCD of DPV assays

Assay order	Scan rate, V/s	Potential step, V	Potential pulse, V	Blocks
1	0.041	0.00750	0.020	1
2	0.019	0.00250	0.060	1
3	0.019	0.0075	0.060	1
4	0.041	0.0025	0.020	1
5	0.041	0.0025	0.060	1
6	0.030	0.0050	0.040	1
7	0.019	0.0075	0.020	1
8	0.030	0.0050	0.040	1
9	0.019	0.0025	0.020	1
10	0.030	0.0050	0.040	1
11	0.041	0.0075	0.060	1
12	0.030	0.0095	0.040	2
13	0.030	0.0050	0.040	2
14	0.030	0.00048	0.040	2
15	0.030	0.0050	0.040	2
16	0.010	0.0050	0.040	2
17	0.030	0.0050	0.040	2
18	0.030	0.0050	0.0038	2
19	0.030	0.0050	0.076	2
20	0.050	0.0050	0.040	2

#### 2.2.2.2. Calibration

To test the experimental conditions selected for the DPV technique, assays were carried out with different concentrations of potassium ferricyanide in order to verify the calibration curve and calculate the detection and quantification limits. These solutions were prepared in 100 mL volumetric flasks, each containing 7.10 g of Na<sub>2</sub>SO<sub>4</sub>, and different amounts of K<sub>3</sub>[Fe(CN)<sub>6</sub>], which concentrations are indicated in the Table 8. Measurements were carried out using 10 mL of each solution mixed with 0.1 mL of KCl 3M and 0.1 mL of acetate buffer.

#### 2.2.3. Metal solutions

Measurements were carried out using 10 mL of each solution, mixed with 0.1 mL of KCl 3M, and 0.1 mL of acetate buffer, in order to verify if the three heavy metals (cadmium, copper and

lead) don't have interferences with each other (independent variables), a study was carried out through DPV analytical tests defined by a full factorial design. Then, the study of the simultaneous analysis of the 3 metals by ASDPV was carried out, followed by tests on wine samples.

*Table 8. Standard calibration solutions of  $K_3[Fe(CN)_6]$*

Solution	$[K_3[Fe(CN)_6]]$ , mg/L
S1	5.113
S2	2.52
S3	1.004
S4	0.503
S5	0.254
S6	0.132
S7	0.08
S8	0.14056
S9	0.1004
S10	0.06024

#### ***2.2.3.1. Full factorial design heavy metals' solutions***

The independency test of the heavy metals' calibrations was evaluated using a full factorial design with 3 factors (Cd, Cu and Pb analysis) and 8 experiments using two levels of concentration (-1 and +1; with no center points). Two intermediate standard solutions of each heavy metal were prepared, the level -1 had a concentration of 34 mg/L (0.5 mL of 1000 mg/L stock solution of the concerned heavy metal diluted to 15 mL) and, the level +1, a final concentration of 100 mg/L (1.0 mL of 1000 mg/L stock solution of the concerned heavy metal diluted to 10 mL). The mixed solutions were prepared by measuring 0.1 mL of the solutions copper, lead, and cadmium of both levels to the electrochemical cell which contained 10 mL of deionized water, 0.1 ml of KCl 3M, and 0.1 mL of acetate buffer according to the full factorial design presented in the Table 9. The final concentrations measured by DPV are also presented in the Table 9.

#### ***2.2.3.2. Heavy metals' standard calibration solutions for ASDPV analysis***

The mixed standard calibration solutions were prepared by diluting 0.1 mL of the stock solution of each heavy metal (1000 mg/L) into several volumetric flasks (50, 100, 250 and 500 mL),

which allowed to establish a calibration curve between 0.20 and 2.0 mg/L for each metal. Each mixed solution analysis was prepared by measuring 10 mL of its volume to the electrochemical cell, which contained 0.1 ml of KCl 3M, and 0.1 mL of acetate buffer.

*Table 9. Mixed solution of the 3 heavy metals accordingly to the full factorial design*

<b>Assay</b>	<b>Cd</b>	<b>Cu</b>	<b>Pb</b>	<b>[Cd<sup>2+</sup>], mg/L</b>	<b>[Cu<sup>2+</sup>], mg/L</b>	<b>[Pb<sup>2+</sup>], mg/L</b>
<b>1</b>	1	-1	-1	0.887	0.302	0.343
<b>2</b>	1	1	-1	0.875	0.890	0.315
<b>3</b>	-1	1	1	0.317	0.902	0.917
<b>4</b>	1	1	1	0.946	0.880	0.982
<b>5</b>	-1	1	-1	0.330	0.929	0.328
<b>6</b>	1	-1	1	0.872	0.312	0.806
<b>7</b>	-1	-1	-1	0.333	0.320	0.318
<b>8</b>	-1	-1	1	0.319	0.315	0.903

### **2.2.3.3. Wine solution for ASDPV analysis**

The wine solution for electrochemical analysis was prepared with a digestion-based method (Zsolt et al., 2008). A volume of 25 mL of a wine sample was added to a digestion glass that was on a hotplate (Heater plate Jouan, Germany) for the water evaporation and reaction with several volumes of H<sub>2</sub>O<sub>2</sub> 30% and of HNO<sub>3</sub> concentrated, which were added to decompose the high organic content of the wine's matrix until a pale-yellow dry residue was obtained. Then, the dry residue was dissolved in 10 mL of deionized H<sub>2</sub>O, 0.1 mL of KCl 3M, and 0.1 mL of acetate buffer for ASDPV analysis.

## **2.3. FLAME SPECTROPHOTOMETER ANALYSIS**

### **2.3.1. Equipment**

The flame atomic absorption spectrophotometer used was a PerkinElmer PinAAcle 900T equipment (Germany) as can be seen in Figure 11.

### **2.3.2. Standard calibration solutions and sample solutions**

Five standard solutions were prepared using the commercial standard solutions of cadmium, copper and lead (1000 mg/L) by dilution (0.25, 0.5, 0.75, 1.0 and 1.5 mL into 50 mL). For copper, the range of concentration achieved was between 0.099 and 0.59 mg/L; for cadmium, it was between 0.099 and 0.59 mg/L; for lead, it was between 0.29 and 1.76 mg/L. The absorbance's results were obtained at the wavelengths of 324.8, 228.8 and 283.3 nm for the heavy metals copper, cadmium and lead, respectively. The calibration zero was settled with deionized water (blank solution).

The wine samples were prepared by dilution of 5 mL of wine into 25 mL, using deionized water.

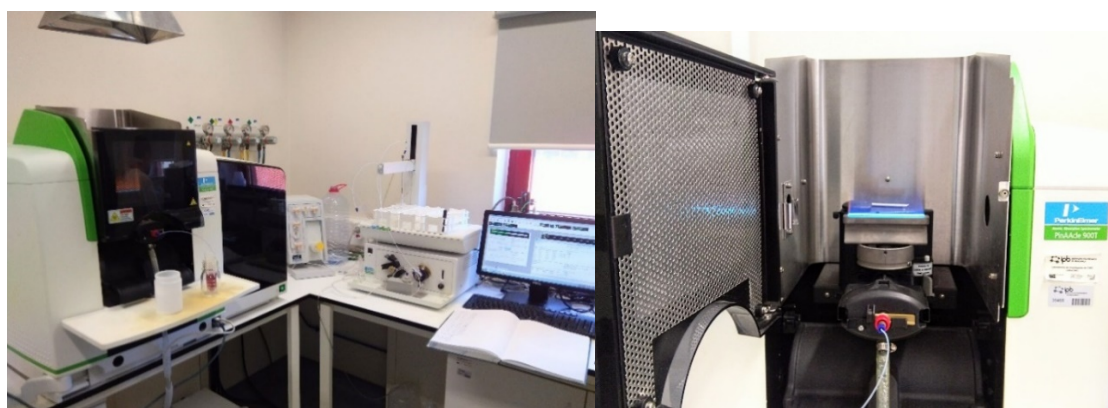


*Figure 11. Flame Atomic absorption spectrophotometer PerkinElmer PinAAcle 900T*

## **2.4. ELECTROTHERMAL SPECTROPHOTOMETER ANALYSIS**

### **2.4.1. Equipment**

In order to achieve a lower detection limit, electrothermal (graphite furnace) atomic absorption spectroscopy (ETAAS) was used together with a digestion of the wine samples. All the ETAAS analysis were performed on the same equipment but, for this experiment, it was equipped with a transversely heated graphite atomizer, incorporating a longitudinal Zeeman-effect background (BC) corrector and an AS-72 autosampler (Perkin-Elmer, Germany). In the THGA, end-capped graphite tubes fitted with integrated graphite platforms (IGPs) (Perkin-Elmer, Part N° B3 000653) were used. For the introduction of sample and modifier solutions, the IGP of the transversely heated graphite atomizer (THGA) was pre-heated at 70 °C. This condition prevented the sputtering and foaming of the organic content of wine samples during

the drying and pyrolysis steps of the graphite furnace heating program, and moreover, it enhanced the reproducibility of the determinations. The details of the graphite furnace heating program are listed in Table 10. Also, the graphite furnace chamber is shown in the Figure 12, as well the graphite tube used.

*Table 10. Graphite furnace heating program*

Step	Temperature (°C)	Ramp time (s)	Hold time (s)	Internal Air flow rate (cm <sup>3</sup> min <sup>-1</sup> )
<b>Drying 1</b>	110	2	30	250
<b>Drying 2</b>	130	10	40	250
<b>Pyrolysis 1</b>	400	10	20	250
<b>Pyrolysis 2</b>	700	10	20	250
<b>Atomization</b>	2200	0	6	0
<b>Cleaning</b>	2450	1	2	250



*Figure 12. Graphite furnace chamber (left figure) and the graphite tube used (right figure)*

#### **2.4.2. Standard calibration solutions and sample solutions**

Four mixed standard solutions were made using the commercial standard solutions of cadmium, copper and lead (1000 mg/L). The concentration of cadmium varied between 25.0 and 99.8 µg/L; copper, between 25.0 and 99.8 µg/L; lead, between 23.9 and 95.6 µg/L. The

absorbance's results were obtained at the wavelengths of 324.8, 228.8 and 283.3 nm for the heavy metals copper, cadmium and lead, respectively. The calibration zero was settled with deionized water (blank solution).

The wine samples were prepared by adding to 5 mL of wine, 1 mL H<sub>2</sub>O<sub>2</sub> 30% and 1 mL of HNO<sub>3</sub> concentrated. After stirring during 1 to 2 min, the final volume was adjusted to 10 mL with deionized water.

## 2.5. STATISTICAL ANALYSIS

Models' validation was performed by checking:

- randomness and normality of the residuals;
- cook's distance (values greater than 1 are indicative that these are excessively influential in the model);
- leverage values (values below 0.2 are acceptable, values between 0.2 and 0.5 are risky and values higher than 0.5 indicate the presence of an influential value or outlier);
- model's p-value (to evaluate the significance of the model obtained using the significance level of 0.05);
- determination coefficient value ( $R^2$ , to verify the amount of variance explained by the model);
- relative standard error (RSE, to confirm the magnitude of the model errors) (Maroco, 2007).

To evaluate the predictive capacity of a model, a simple linear regression model was established between the concentrations predicted by the model and the experimental values. The results are considered satisfactory if the linear regression parameters are close to the theoretical values (Roig and Thomas, 2003; Costa Arca et al., 2019): "zero" (0) for root square error (RSE) and intercept; "one" (1) for slope and the determination coefficient ( $R^2$ ).

Also, the confidence interval at 95% of the slope and intercept can be used to confirm that statistically they could be regarded as the theoretic values of "one" and "zero", respectively.

### 3. RESULTS AND DISCUSSION

The graphite composite working electrode tested in this study had the composition of 50% composite graphite and 50% Araldite glue and was tested in its performance in the analysis of a redox solution of  $K_3[Fe(CN)_6]$  containing the electrolyte  $Na_2SO_4$ , in order to verify its behavior varying several parameters of the CV and DPV techniques. Also, as the main purpose, it was used for the analysis of three heavy metals (cadmium, copper and lead) in wine by applying ASDPV technique.

#### 3.1. REDOX SOLUTION

##### 3.1.1. Cyclic voltammetry

###### 3.1.1.1. Reversibility of redox reaction

In Figure 13, the cyclic voltammogram shows how the cathodic peak current ( $I_{pc}$ ) and anodic peak current ( $I_{pa}$ ) were measured in the potential range of -0.4 to 1.0 V, in long with anodic peak potential ( $E_{pa}$ ) and cathodic peak potential ( $E_{pc}$ ).

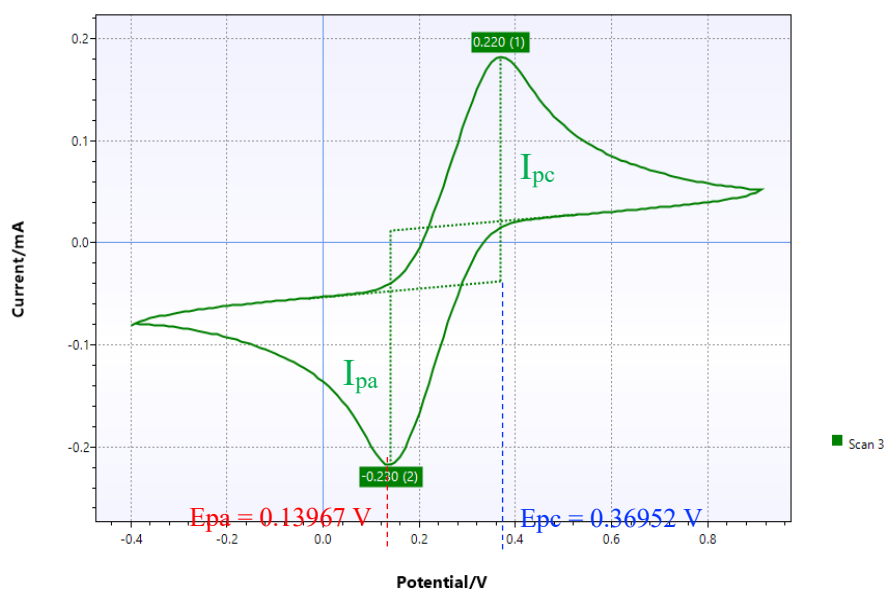


Figure 13. Cyclic voltammogram obtained for the redox solution with the lab-made graphite composite working electrode.  $E_{pa}$ - anodic peak potential;  $E_{pc}$ - cathodic peak potential;  $I_{pa}$ - anodic peak current;  $I_{pc}$ - cathodic peak current.

In Figure 14 is presented all the cyclic voltammograms of the solution of 0.01M  $K_3[Fe(CN)_6]$  and 0.5M  $Na_2SO_4$  analysed accordingly to the CCD experimental design with 2 factors (scan rate and potential step) and 14 assays. The mean values of  $E_{pa}$  and  $E_{pc}$  were of  $0.36\pm 0.01$  V and  $0.16\pm 0.01$  V, respectively. After calculating the half wave potential ( $E_{1/2}$ ), the mean value was estimated at  $0.260\pm 0.002$  V. This equality confirms the reversibility of the redox solution. The  $I_{pa}$  and  $I_{pc}$  values varied in the interval of 110.0 to 240.1  $\mu A$  and 112.5 to 249.6  $\mu A$ , respectively, showing similar results between them.

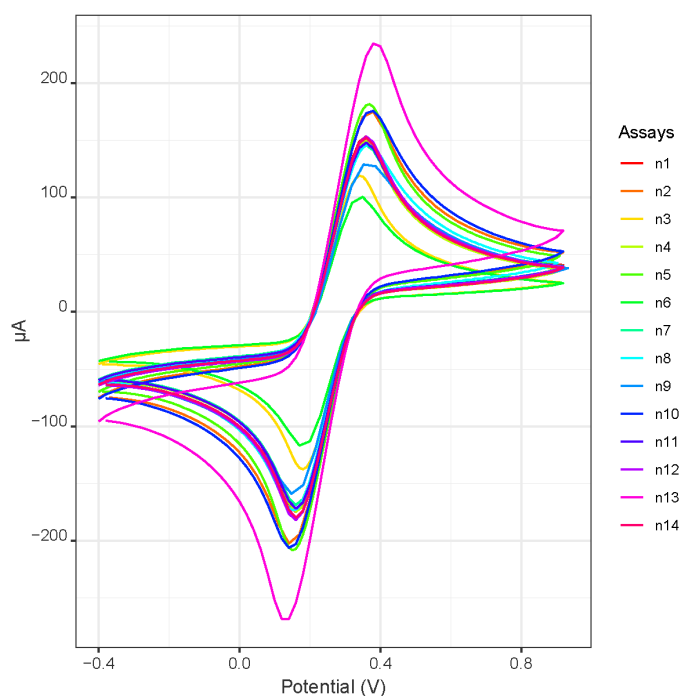


Figure 14. All cyclic voltammograms from the applied CCD with 2 factors

Also, the ratio  $I_{cp}/I_{ap}$  had a mean value of  $1.030\pm 0.006$  and a percentage relative standard deviation (RSD%) of 0.63%, meaning that the working electrode is precise in the voltammetric analysis. The representation of this ratio (Figure 15) showed the expected linear tendency of a reversible redox solution. The linear equation had a slope of  $1.053\pm 0.007$ , an intercept of  $-4.1\pm 1.2$  and a correlation coefficient of 0.9998. Considering the figure and results, the working electrode had a good performance in the CV.

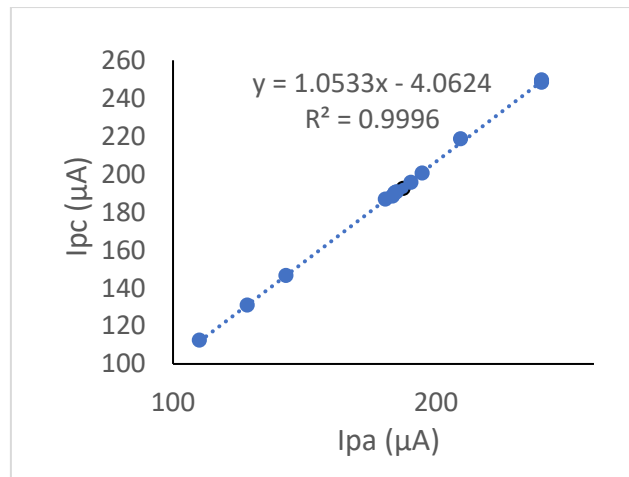


Figure 15. Linear relation between  $I_{pc}$  and  $I_{pa}$

### 3.1.1.2. Response surface methodology

The performance of the working electrode in the analysis with CV was evaluated using a CCD with two factors: scan rate (level -1 = 0.0029 V/s; level +1 = 0.17 V/s) and  $E_{pulse}$  (level -1 = 0.0058 V; level +1 = 0.34 V). The  $I_{cp}$  results (varied between 112.5 and 249.6  $\mu\text{A}$ ) obtained from the voltammograms, shown in Figure 14, were treated using the RSM technique, considering a model where the main, interaction and squared effects were tested. Globally, RSD% values of each CV assay were lower than 5%, which is acceptable. Table 11 presents the terms with significance at 0.05% level. As can be seen, the working electrode in the CV analysis had dependency of the scan factor and not  $E_{pulse}$ , in the conditions tested. The final model has the following equation

$$I_{cp} = 88.2224 + 1366.5933 \times \text{Scan\_rate} - 769.0232 \times E_{pulse} - 2304.4203 \times \text{Scan\_rate}^2,$$

being a significant model with  $p\text{-value} < 0.001$ , which explains 98.6% of data variability (determination coefficient of 0.986). The results in Table 11 show that the main effects of scan rate and potential step were significant parameter for cyclic voltammetry results, as well as the squared term of scan rate, since  $p\text{-value} < 0.05$ . So, there is no evidence of interaction between the two factors.

The model's quality can be evaluated by considering its residues (predicted performance). Figure 16 shows several plots that allows to verify that the model obtained was satisfactory since it meets the regression assumptions validation. It shows that residuals have a random

behavior, are normally distributed since the vast majority of residuals follow a straight line and there are no significant influential cases, because all cases are well inside of the Cook's distance lines and have leverage values lower than 0.6.

Table 11. RSM final model from response Icp obtained from the cyclic voltammograms

Source	Estimate	Std Error	P-value
<b>Intercept</b>	88.2224	8.6147	<0.001 ***
<b>Scan rate</b>	1366.5933	162.4381	<0.001 ***
<b>Epulse</b>	-769.0232	185.9445	<0.01 **
<b>(Scan rate)<sup>2</sup></b>	-2304.4203	793.2794	<0.05 *

Signif.codes: 0 '\*\*\*' 0.001 '\*\*' 0.01 '\*' 0.05 '.' 0.1 ' ' 1

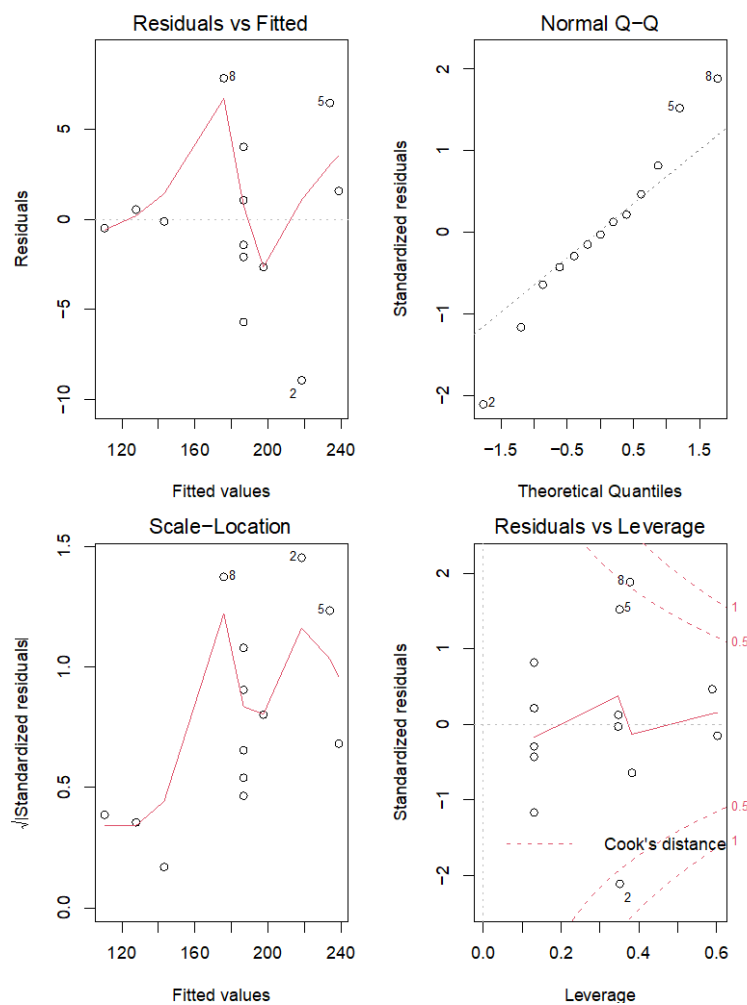


Figure 16. CV-RSM model residuals' plots of: residuals vs fitted; normal Q-Q; standardize residuals vs fitted values; standardized residual vs leverage, including cook's distance limits

The 3D surface plot of the  $I_{cp}$  values (CV response) in function of the two factors scan rate and  $E_{pulse}$  is shown in Figure 17.

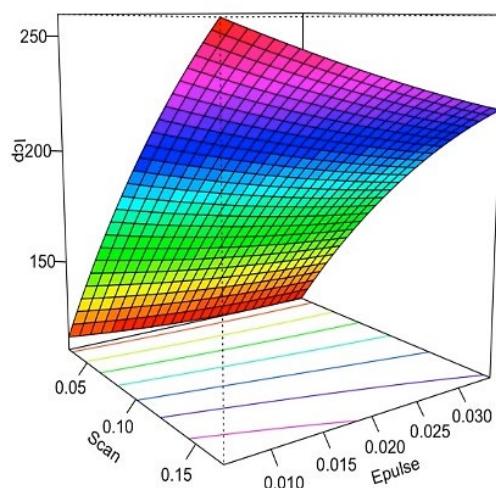


Figure 17. 3D surface plot of the  $I_{cp}$  values (CV response) in function of the two factors scan rate and potential pulse

### 3.1.2. Differential pulse voltammetry

#### 3.1.2.1. Response surface methodology

The performance of the working electrode in the analysis by DPV was evaluated using the experimental CCD with three factors: scan rate (level -1 = 0.01 V/s; level +1 = 0.05 V/s), potential pulse (level -1 = 0.0038 V; level +1 = 0.076 V) and potential step (level -1 = 0.00048 V; level +1 = 0.0095 V). Figure 18 shows the typical differential pulse voltammogram (measured in the potential range of -1.0 to 1.0 V) obtained for the redox solution (0.01M  $K_3[Fe(CN)_6]$  with 0.5M  $Na_2SO_4$ ), from the CCD assays and the peak current intensity variation ( $\Delta I_p$ ) that was used as the experimental design response. The CCD assays allowed to study the main, interaction and squared effects of the three factors tested, being all voltammograms represented in the Figure 19. The  $\Delta I_p$  values varied between 8.1 to 166.6  $\mu A$  and were measured at the potential value of  $0.479 \pm 0.001$  V.

Generally, RSD% of assays were  $>5$  and  $\leq 10\%$ , which is acceptable, and some were  $>0.1$  and  $\leq 1\%$  which is considered good. Table 12 presents the terms with significance at 0.05% level, showing dependency of scan rate and potential pulse in the DPV analysis as obtained in the tests with CV, but without significance in the square term of the scan rate factor.

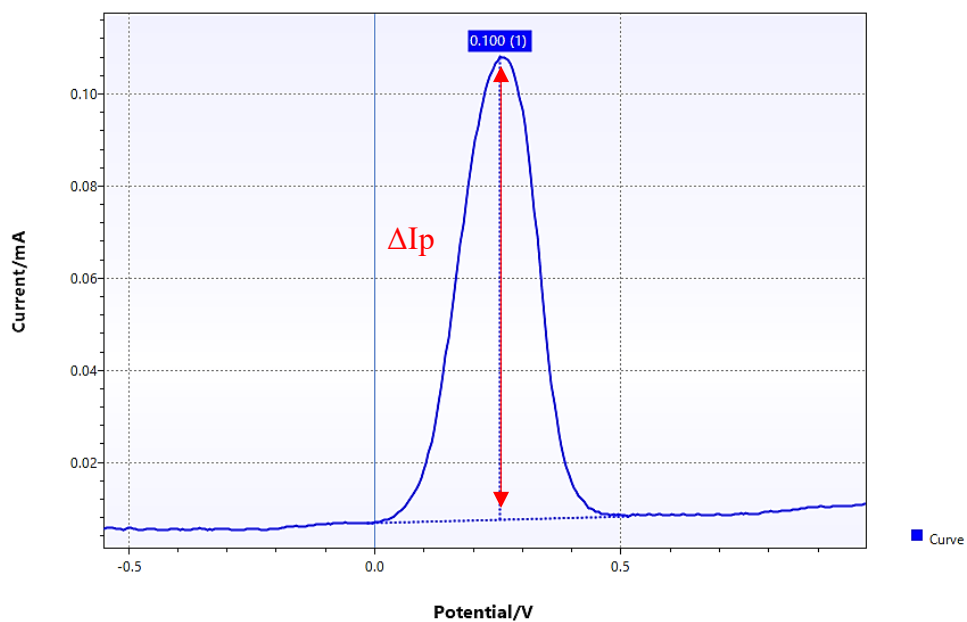


Figure 18. Differential pulse voltammogram obtained for the redox solution with the lab-made graphite composite working electrode

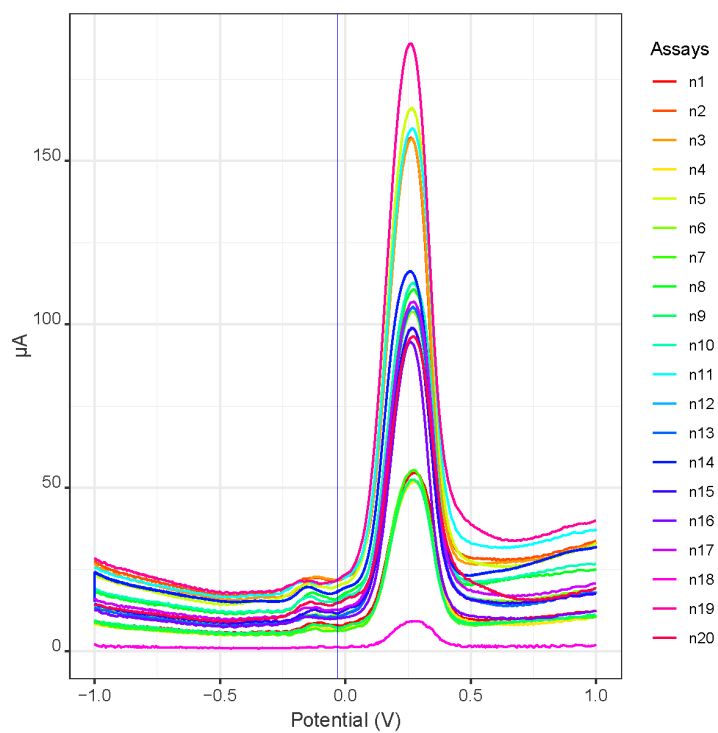


Figure 19. All differential pulse voltammograms from the applied CCD with 3 factors

Table 12. RSM final model from response  $\Delta I_p$  obtained from the differential pulse voltammograms

Source	Estimate	Std Error	P-value
Intercept	12.3595	6.1581	>0.05
<b>Scan rate</b>	-327.2403	142.4761	<0.05 *
Estep	270.5585	636.2109	>0.05
<b>Epulse</b>	2199.9008	79.2971	<0.001 ***

Signif.codes: 0 '\*\*\*' 0.001 '\*\*' 0.01 '\*' 0.05 '.' 0.1 ' ' 1

So, the final model has the following equation (without the term Estep which was not significant)

$$\Delta I_p = 13.6 + 2199.9 \times E_{\text{pulse}} - 322.8 \times \text{scan rate},$$

being a significant model with p-value < 0.001, which explains 97.95% of data variability (determination coefficient of 0.98). The model's quality can be evaluated by considering its residues (predicted performance). Figure 20 shows several plots that allows to verify that the model obtained was satisfactory since it meets the regression assumptions validation. It shows that residuals have a random behavior, are normally distributed since the vast majority of residuals follow a straight line and there are no significant influential cases, because all cases are well inside of the Cook's distance lines and have leverage values lower than 0.7. Therefore, the working electrode had a good performance in the differential pulse voltammetry as well.

The 3D surface plot of the  $\Delta I_p$  values (DPV response) in function of the three factors scan rate, Estep and Epulse is shown in Figure 21.

The conditions selected from these two RSM studies were 0.03 V/s for the scan rate, 0.01 V for the step potential, and 0.04 V for the pulse potential for DPV. While for CV, 0.1 V/s was selected for scan rate, and 0.015 V for step potential.

For testing the DPV conditions, a calibration procedure was applied using several standard solutions of potassium ferricyanide.

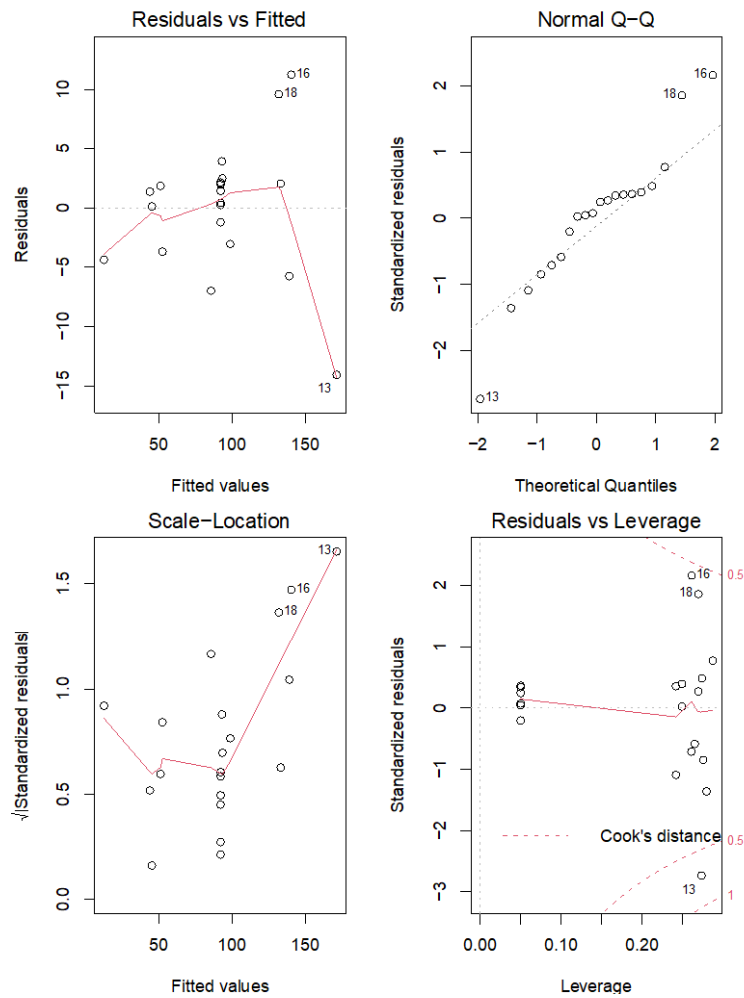


Figure 20. DPV-RSM model residuals' plots of: residuals vs fitted; normal Q-Q; standardize residuals vs fitted values; standardized residual vs leverage, including cook's distance limits

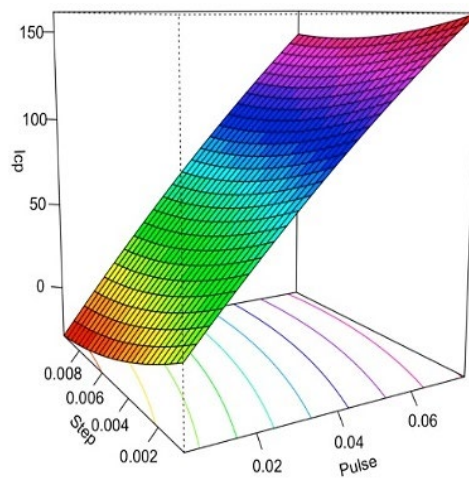


Figure 21. 3D surface plot of the DPV response  $\Delta I_p$  values in function of the two factors scan rate and potential pulse

### 3.1.2.2. Calibration with potassium ferricyanide solutions

To verify the DPV response performance of the working electrode, 7 standard solutions of  $K_3[Fe(CN)_6]$  (with 0.5M  $Na_2SO_4$ ) were prepared in the concentration range of 0.080 to 5.11 mg/L. It was shown that it was possible to establish a linear model within the minimum concentration of 0,13 mg/L. The linear regression between the maximum current intensity measured in each peak (varied between 12.5 and 107.7  $\mu A$ ) and the respective logarithm of the concentration of  $K_3[Fe(CN)_6]$  gave a slope of  $60\pm 2 \mu A$ , intercept of  $65.1\pm 0.9 \mu A$  and correlation coefficient of 0.9985 (model with p-value < 0.001). The calculated limit of detection and quantification was of 0.05 and 0.15 mg/L, respectively. These limits can be improved in accuracy with more assays for reducing the calibration errors and increase the correlation coefficient. The Figure 22 presents the plot of the linear relation obtained from the calibration using the peak maximum current intensity and the logarithm of the concentration of  $K_3[Fe(CN)_6]$ , highlighting the point corresponding to the lowest concentration (0.08 mg/L, lower than the limit of quantification) with another color as it is not within the dynamic range of the DPV analysis.

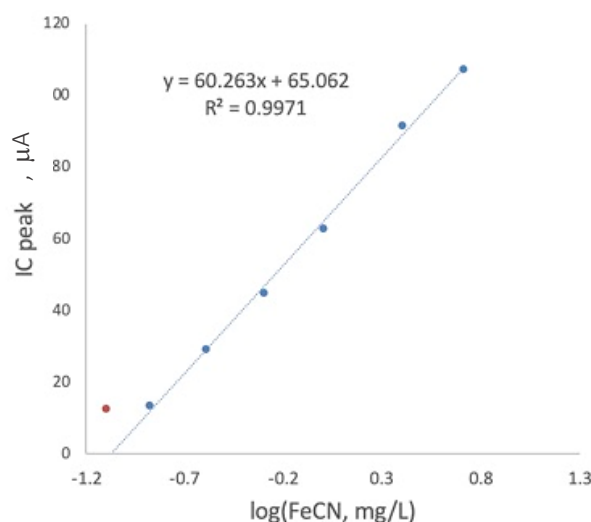


Figure 22. Calibration curve with  $K_3[Fe(CN)_6]$  solutions containing 0.5M  $Na_2SO_4$

The results presented seem to show that the working electrode made in the lab has an acceptable performance and, therefore, it can be applied in the analysis of heavy metals.

## 3.2. HEAVY METALS ANALYSIS

The 3 heavy metals studied in this work are cadmium, copper and lead. The results referring to the analysis of standard solutions and wine samples by the instrumental analytical techniques, FAAS, ETAAS, DPV and ASDPV are presented below.

### 3.2.1. Flame spectrophotometric analysis

#### 3.2.1.1. Cadmium, copper and lead calibration curves

The Figure 23 presents the calibrations curves obtained for the analysis of the three heavy metals, copper, cadmium, and lead using flame atomic absorption spectrophotometer, referring the wavelengths used in each measurement. The three calibration curves exhibited a linear behavior between the absorbances and the concentrations of the standard solutions of cadmium, copper and lead (Table 13). The determination coefficients ( $R^2$ ) showed that, in general, the obtained models explained more than 99% of the data variability (correlation coefficients higher than 0.998). However, the linear model for cadmium analysis had higher sensitivity (slope of 0.36) followed by the copper analysis (slope of 0.19) and, at last, the lead analysis (slope of 0.017). Overall, acceptable linear relationships were obtained for copper, cadmium and lead analysis, which were applied in the analysis of 8 wine samples using FAAS.

Table 13. Cadmium, copper and lead calibration curves results

Metal	Range, mg/L	Slope, L/mg	Intercept	R	LD, mg/L	LQ, mg/L
Cd <sup>2+</sup>	0.099; 0.591	0.363 ( $\pm 0.005$ )	-0.002 ( $\pm 0.002$ )	0.9996	0.015	0.046
Cu <sup>2+</sup>	0.099; 0.592	0.188 ( $\pm 0.001$ )	0.0004 ( $\pm 0.0003$ )	0.99990	0.006	0.019
Pb <sup>2+</sup>	0.294; 1.761	0.0170 ( $\pm 0.0006$ )	-0.0005 ( $\pm 0.0004$ )	0.9983	0.081	0.245

#### 3.2.1.2. Wine analysis

The results from FAAS analysis showed that only the wines R1, W1, W2 and W4 presented quantifiable levels for copper (Table 14), being satisfactory results in precision since the respective percentage of relative standard deviation were lower than 5.1%. The other heavy

metals were not detected in all wine samples by this analytical technique. Due to these results, the wine samples were also analyzed by furnace (graphite chamber), using ETAAS.

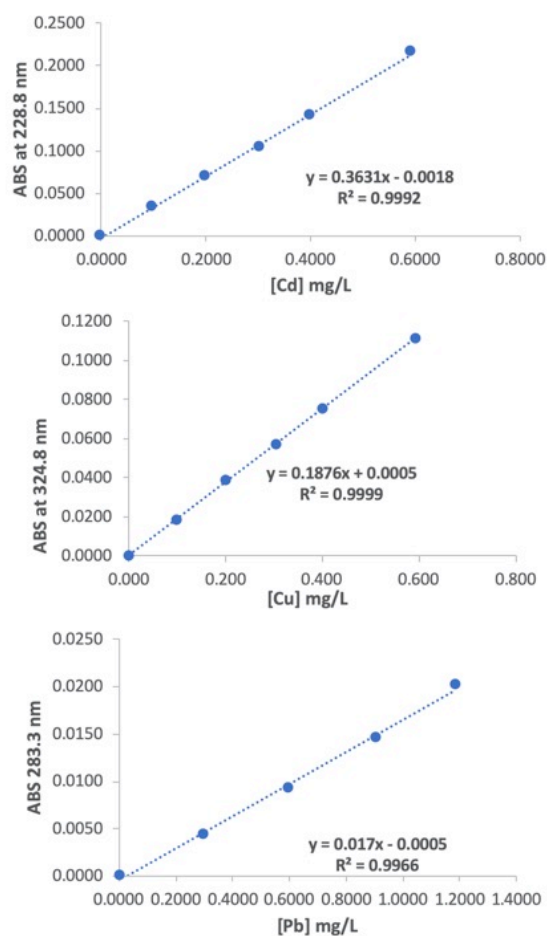


Figure 23. Calibration curve for cadmium, copper and lead obtained using FAAS

Table 14. Heavy metal concentrations in wine by FAAS analysis \*

Sample	[Cd <sup>2+</sup> ], mg/L	[Cu <sup>2+</sup> ], mg/L	[Pb <sup>2+</sup> ], mg/L
R1	nd	0.416 (±0.005)	nd
R2	nd	nd	nd
R3	nd	nd	nd
R4	nd	nd	nd
W1	nd	0.291 (±0.007)	nd
W2	nd	0.226 (±0.009)	nd
W3	nd	nd	nd
W4	nd	0.176 (±0.009)	nd

\*) nd – not detected

### 3.2.2. Electrothermal spectrophotometric analysis

The Figure 24 presents the calibrations curves obtained for the analysis of the three heavy metals, copper, cadmium, and lead using ETAAS, using the same wavelengths applied in FAAS analysis. The three calibration curves exhibited a linear behavior between the absorbances and the concentrations of the standard solutions of cadmium, copper and lead, being the linear regression parameters presented in Table 15. The determination coefficients ( $R^2$ ) were acceptable and slightly lower than those obtained using FAAS, for cadmium and copper. Globally, the obtained models explained more than 99% of the data variability (correlation coefficients higher than 0.9985). However, the linear model for cadmium analysis had higher sensitivity (slope of 0.032) followed by the copper analysis (slope of 0.0046) and, at last, the lead analysis (slope of 0.00214). The ETAAS sensitivity was higher than the FAAS, considering that the concentrations were not in the same units. Overall, acceptable linear relationships were obtained for copper, cadmium and lead analysis, which were applied in the analysis of 8 wine samples using ETAAS. This methodology allowed to analyse samples at lower trace levels than the FAAS.

*Table 15. Cadmium, copper and lead calibration curves results*

Metal	Range, $\mu\text{g/L}$	Slope, L/mg	Intercept	R	LD, $\mu\text{g/L}$	LQ, $\mu\text{g/L}$
$\text{Cd}^{2+}$	0.054; 0.181	0.032 ( $\pm 0.001$ )	0.005 ( $\pm 0.004$ )	0.9976	0.45	1.36
$\text{Cu}^{2+}$	0.136; 0.463	0.0046 ( $\pm 0.0001$ )	0.011 ( $\pm 0.004$ )	0.9988	2.77	8.61
$\text{Pb}^{2+}$	0.060; 0.206	0.00214 ( $\pm 0.00004$ )	0.004 ( $\pm 0.003$ )	0.9989	4.08	12.63

#### 3.2.2.2. Wine analysis

The results from wine analysis with ETAAS are presented in Table 16. With this analytical method was possible to quantify concentration levels of copper in all wine samples. However, no levels of cadmium and lead were detected in the samples. The concentration results RSD% values lower than 6.0 %. The R1 sample had the highest copper concentration, followed by W1 and W2 samples. The lowest copper concentration was obtained in the R2 sample, followed by the W3 and R4 samples. These concentrations were, in average, 1.2 times higher than those that were quantified by the FAAS methodology.

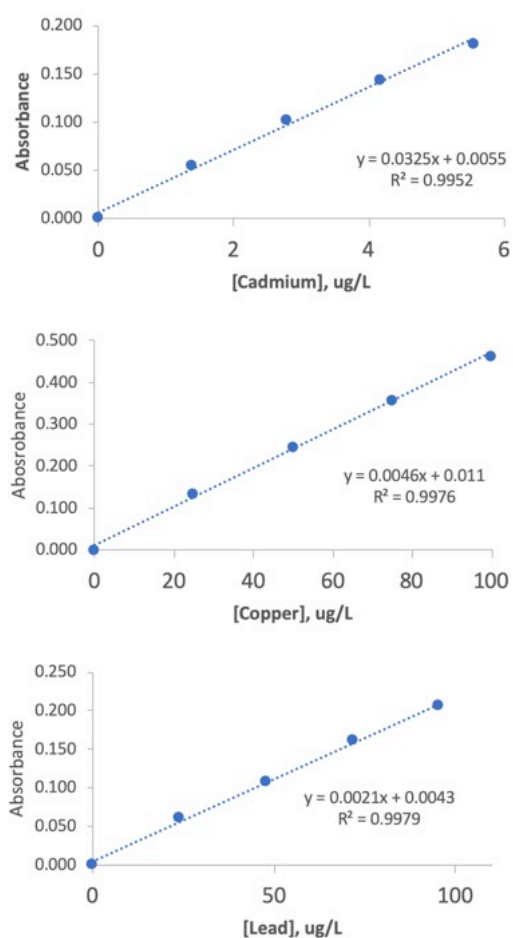


Figure 24. Calibration curve for cadmium, copper and lead obtained using ETAAS

Table 16. Heavy metal concentrations in wine by ETAAS analysis \*

Sample	[Cd <sup>2+</sup> ], mg/L	[Cu <sup>2+</sup> ], mg/L	[Pb <sup>2+</sup> ], mg/L
R1	nd	0.535 (±0.002)	nd
R2	nd	0.011 (±0.002)	nd
R3	nd	0.075 (±0.002)	nd
R4	nd	0.053 (±0.002)	nd
W1	nd	0.452 (0.007)	nd
W2	nd	0.352 (0.009)	nd
W3	nd	0.048 (±0.002)	nd
W4	nd	0.173 (0.009)	nd

\*) nd – not detected

As can be seen, the copper concentrations in the samples varied between 0.011 and 0.535 mg/L, being in accordance with the OIV regulation since the obtained levels were lower than 1.0 mg/L (MAL, Maximum Acceptable Levels).

### **3.2.3. Electrochemical analysis**

#### ***3.2.3.1. DPV calibrations independency***

For testing the independence between the calibrations of each metal, a full factorial design with 8 assays and with two concentration levels (approximately, 0.3 and 0.9 mg/L) for each metal was applied. The main and interaction effects were tested and results showed that the terms of the interactions were not significant and that, for each heavy metal, only the respective main factor was significant, indicating that the calibrations will be independent between the 3 analyzed metals. Table 17 shows the main effects terms together with the standard errors and p-values, as well as, the determination coefficient and p-value of each model. All the models had acceptable determination coefficient ( $R^2 \geq 0.91$ ) and were significant (p-values  $\leq 0.014$ ). Regarding the assumptions validation to evaluate each model's quality, an acceptable performance was obtained. The residuals have a random behavior, are normally distributed and there were no significant influential cases since, the Cook's distances and leverage values were lower than 1 and 0.6, respectively.

#### ***3.2.3.2. ASDPV calibrations***

Considering the low concentrations obtained from the analysis of wine samples by ETAAS, the present study focused on the application of the ASDPV technique, having tested the deposition step in two times: 2 and 4 minutes. For the ASDPV analysis with 2 and 4 min of deposition, voltammograms of three mixed heavy metals standard solutions, with concentrations approximately to 2.0, 1.0 and 0.4 mg/L, are presented in Figure 25. The peak of  $\text{Cd}^{2+}$  appears at mean potential  $-0.76 \pm 0.01$  V,  $\text{Pb}^{2+}$  at potential  $-0.47 \pm 0.02$  V and  $\text{Cu}^{2+}$  at  $-0.10 \pm 0.03$  V. The voltammograms showed a similar profile, noting that with the deposition step of 4 min, the peaks are higher, as expected.

Table 17. Models with the main effects for each heavy metal calibration

Source	Estimate	Std Error	P-value
<b>Cadmium calibration (<math>R^2 = 0.97</math>; p-value = 0.002)</b>			
<b>Intercept</b>	10.65424	0.67595	<0.001 ***
<b>[Cd<sup>2+</sup>]</b>	7.63165	0.67595	<0.001 ***
<b>Cu<sup>2+</sup>]</b>	-0.17218	0.67595	>0.05
<b>[Pb<sup>2+</sup>]</b>	1.00065	0.67595	>0.05
<b>Copper calibration (<math>R^2 = 0.91</math>; p-value = 0.014)</b>			
<b>Intercept</b>	5.49062	0.40825	<0.001 ***
<b>[Cd<sup>2+</sup>]</b>	-0.38874	0.40825	>0.05
<b>Cu<sup>2+</sup>]</b>	2.59446	0.40825	<0.01 **
<b>[Pb<sup>2+</sup>]</b>	0.16672	0.40825	>0.05
<b>Lead calibration (<math>R^2 = 0.94</math>; p-value = 0.007)</b>			
<b>Intercept</b>	19.50652	1.48200	<0.001 ***
<b>[Cd<sup>2+</sup>]</b>	2.68327	1.48200	>0.05
<b>Cu<sup>2+</sup>]</b>	0.71739	1.48200	>0.01
<b>[Pb<sup>2+</sup>]</b>	11.38228	1.48200	<0.01 **

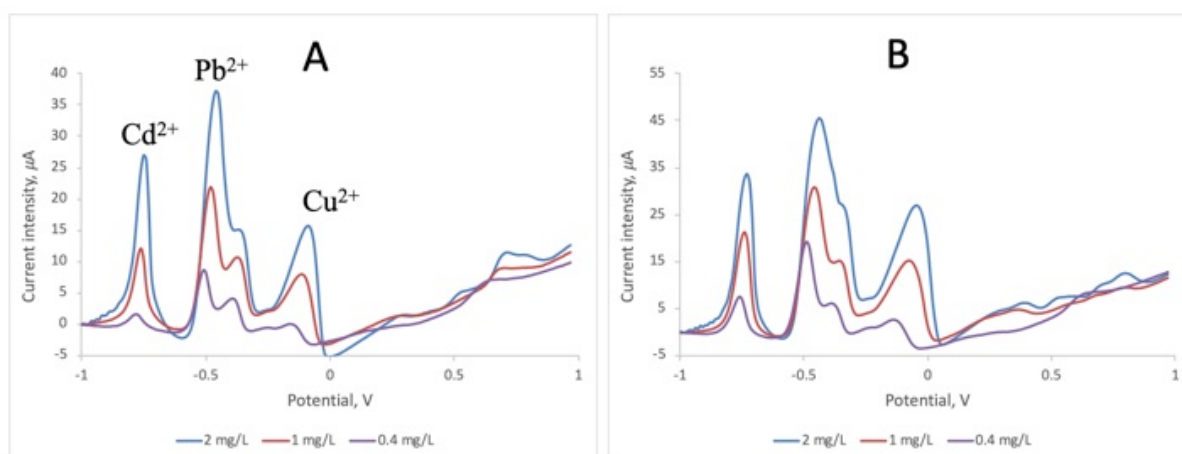


Figure 25. ASDPV voltammograms of three standard solutions of calibration obtained using: (A) 2 min of deposition and (B) 4 min of deposition

In Figure 26, the calibration curves for the three heavy metals are presented, considering that the anodic stripping technique was performed with step deposition of 2 or 4 minutes.

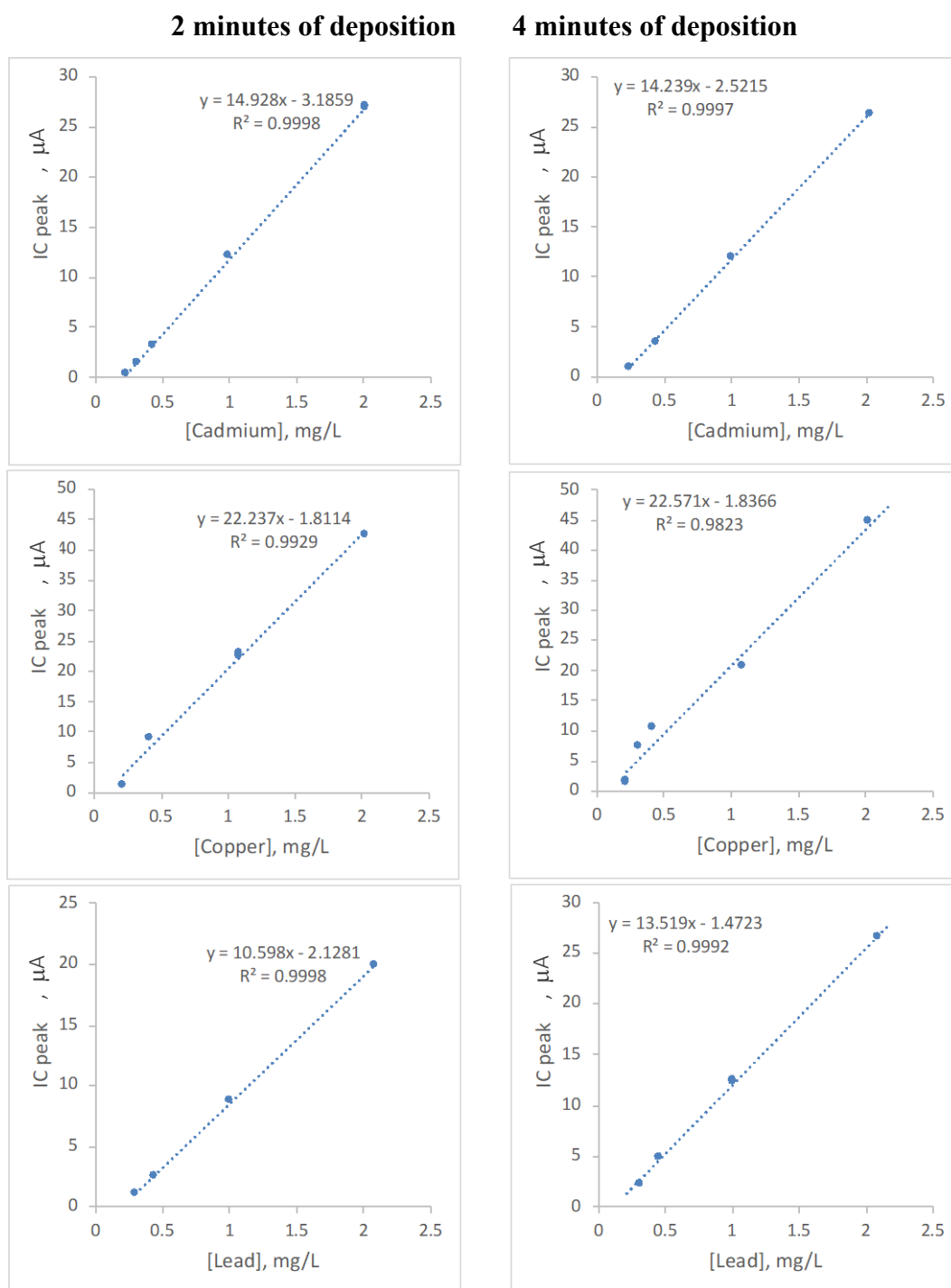


Figure 26. Calibration curve for cadmium, copper and lead obtained using ASDPV with 2 and 4 min of deposition

Table 18 shows concentration range of the mixed heavy metals standard solutions of calibration and the calibration curve parameters obtained, for both two times of step deposition.

Table 18. Calibration curve parameters obtained from the analysis of the three metals by ASDPV with 2 and 4 min of deposition \*

Metal	Range, mg/L	Slope, L/(mg.μA)	Intercept, μA	R	LD, mg/L	LQ, mg/L
<b>Anodic stripping with 2 minutes</b>						
Cd <sup>2+</sup>	0.235; 2.02	14.9 (±0.1)	-3.2 (±0.1)	0.99989	0.031	0.093
Cu <sup>2+</sup>	0.221; 2.02	22.2 (±1.1)	-1.8 (±1.2)	0.993	0.187	0.565
Pb <sup>2+</sup>	0.305; 2.08	10.6 (±0.1)	-2.1 (±0.1)	0.99988	0.044	0.132
<b>Anodic stripping with 4 minutes</b>						
Cd <sup>2+</sup>	0.235; 2.02	14.2 (±0.2)	-2.5 (±0.2)	0.9998	0.048	0.144
Cu <sup>2+</sup>	0.221; 2.02	23.0 (±1.6)	-2.0 (±2.3)	0.993	0.236	0.714
Pb <sup>2+</sup>	0.305; 2.08	13.5 (±0.2)	1.5 (±0.2)	0.9996	0.061	0.186

\*) R – correlation coefficient; LD – limit of detection; LQ – limit of quantification

The results showed that the ASDPV technique, using 2 and 4 min as deposition step, allowed to obtain a linear behavior between the peak current intensity variation ( $\Delta I_p$ ) and the concentrations of Cd<sup>2+</sup>, Cu<sup>2+</sup> and Pb<sup>2+</sup> ions. The determination coefficients ( $R^2$ ) showed that, in general, the obtained models explained more than 98% of the data variability (correlation coefficients higher than 0.993) for both deposition times of anodic stripping. The linear models for Cd<sup>2+</sup>, Cu<sup>2+</sup> and Pb<sup>2+</sup> analysis have similar sensitivities between the two times of the deposition step. The linear relationships were acceptable but further assays could improve these results, mainly in the ASDPV analysis of Cu<sup>2+</sup> with 2 and 4 min of deposition step (correlation coefficients of 0.993), by reducing the errors of the linear regression parameters. However, in future work, assays will be carried out to experimentally determine the LDs and LQs, since the calculated ones are dependent on the errors present in the models.

Other researchers have shown lower LD values, also using the ASDPV technique: Lin et al. (2014) obtained LD values for cadmium, lead, and copper of 0.10, 0.20, and 0.45 μg/L, respectively, using a modified glassy carbon as working electrode; Cesarino et al. (2009) had LD values of 1.12, 0.32, and 0.062 μg/L for cadmium, copper and lead, respectively, using a composite graphite as working electrode; Antunovic et al. (2020) obtained 23.6 and 5.5 μg/L for copper and lead, respectively, with a modified glassy carbon as WE.

Globally, the WE showed an acceptable sensitivity towards the heavy metal analysis, leading to test its performance on wine analysis.

### 3.2.3.3. ASDPV analysis of wine

The ASDPV results from the analysis of eight wine samples are shown in Table 19. As expected, considering the analytical results obtained by ETAAS, it was only detected the presence of copper and at levels that could be quantified (Figure 27). The copper peaks in wine analysis appeared at the potential of  $-0.03 \pm 0.02$  V, which is close to the potential of the copper peaks obtained with the calibration mixture solutions ( $-0.10 \pm 0.03$  V).

Overall, the analytical errors were between the values of 0.03% and 14.1%, considered acceptable because the copper concentrations in the samples are trace levels, which ranged between 0.08 and 0.55 mg/L ( $1.2 \times 10^{-6}$  mol/L and  $8.6 \times 10^{-6}$  mol/L, respectively). The results from ASDPV analysis with 4 min of deposition were higher 1.7 times than those from 2 min of deposition, as can be seen in Figure 28.

Table 19. Heavy metal concentrations in wine by ASDPV analysis \*

Sample	[Cu <sup>2+</sup> ], mg/L	[Cd <sup>2+</sup> ], mg/L	[Pb <sup>2+</sup> ], mg/L
<b>Anodic stripping with 2 minutes of deposition</b>			
R1	0.36 ( $\pm 0.05$ )	nd	nd
R2	0.08 ( $\pm 0.01$ )	nd	nd
R3	0.097 ( $\pm 0.002$ )	nd	nd
R4	0.104 ( $\pm 0.006$ )	nd	nd
W1	0.26 ( $\pm 0.02$ )	nd	nd
W2	0.2201 ( $\pm 0.0008$ )	nd	nd
W3	0.132 ( $\pm 0.008$ )	nd	nd
W4	0.10 ( $\pm 0.01$ )	nd	nd
<b>Anodic stripping with 4 minutes of deposition</b>			
R1	0.55 ( $\pm 0.02$ )	nd	nd
R2	0.09 ( $\pm 0.01$ )	nd	nd
R3	0.137 ( $\pm 0.009$ )	nd	nd
R4	0.12 ( $\pm 0.01$ )	nd	nd
W1	0.506 ( $\pm 0.009$ )	nd	nd
W2	0.3608 ( $\pm 0.006$ )	nd	nd
W3	0.10 ( $\pm 0.01$ )	nd	nd
W4	0.20 ( $\pm 0.02$ )	nd	nd

\*) nd – not detected

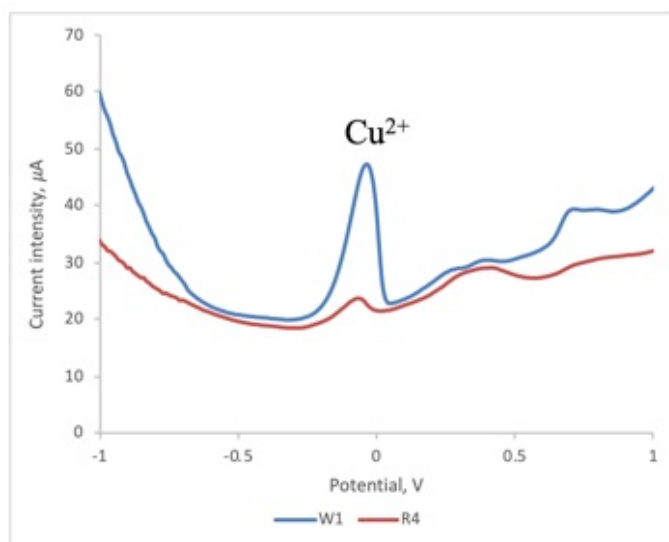


Figure 27. ASDPV voltammograms with 4 min of deposition of samples W1 and R4

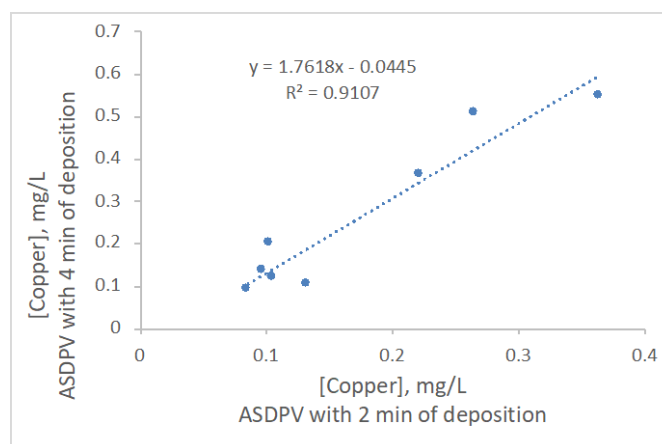
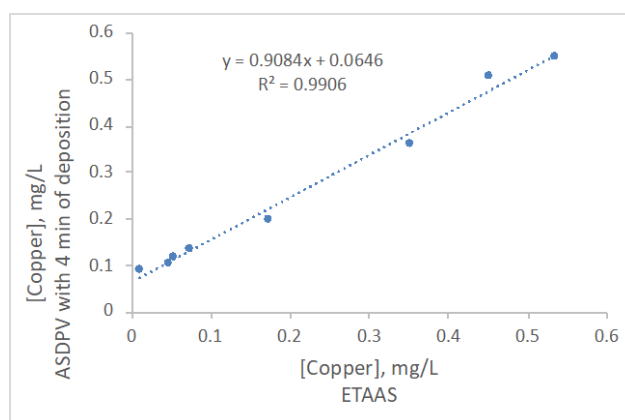


Figure 28. Linear relation between wine's  $\text{Cu}^{2+}$  concentrations obtained with ASDPV analysis with 4 min of deposition vs. 2 min of deposition

These results are showing that there is a need to optimize the ASDPV analyzes at the procedural level in order to reduce the experimental errors (to guarantee the precision and accuracy of the analyses) such as, for example, avoiding the additive volumes of the acetate buffer solution and the KCl electrolyte to the solution to be analyzed and simply carry out the analysis with fixed volume of a mixed solution.

From the comparison with the results obtained by ETAAS, it was verified that the analytical data of ASDPV with 4 min of deposition present the best correlation, as can be seen in Figure 29. The  $\text{Cu}^{2+}$  concentrations in wine obtained by ASDPV analysis were lower 0.9 times than those from ETAAS analysis. According to OIV the allowed maximum concentration of copper is 1000  $\mu\text{g/L}$  and, as it can be seen, all concentrations obtained were lower than those allowed

by OIV, meaning that the Portuguese and Spanish wines analyzed showed quality in terms of copper concentration levels.



*Figure 29. Linear relation between wine's  $\text{Cu}^{2+}$  concentrations obtained with ASDPV analysis with 4 min of deposition vs. ETAAS analysis*

The copper concentration levels obtained in the present work are in accordance with three recent published articles that used the ASDPV technique for copper analysis: Antunovic et al. (2020) declared the determination of copper in wine with concentrations ranging between 36.2 and 168  $\mu\text{g/L}$  (0.0362 and 0.168 mg/L, respectively) for different wines using a modified glassy carbon electrode as a working electrode; Brainina et al. (2004) quantified copper concentrations between 58 and 519  $\mu\text{g/L}$  (0.058 mg/L and 0.519 mg/L, respectively) in different samples of wine with a thick-film modified graphite-containing electrode; Maciel et al. (2019) obtained concentrations within the range of 81.4 up to 105.9  $\mu\text{g/L}$  (0.0814 mg/L and 0.1059 mg/L, respectively) for different types of wines, using a platinum wire as WE.

## CONCLUSIONS

This work aimed to develop an electrochemical cell with a lab-made graphite composite working electrode to analyze cadmium, copper and lead ions in wine, because they can be toxic above the maximum acceptable levels.

The working electrode's performance was tested using a reversible redox solution of  $K_3[Fe(CN)_6]$  with response surface methodology, showing the CV dependency with scan rate and potential step, as well as with the squared term of scan rate. The DPV revealed dependency only with scan rate and potential pulse. Within the space defined for the experiments, CV and DPV proved to be applicable. For the DPV metal analysis work, the conditions selected were 0.03 V/s for the scan rate, 0.01 V for the step potential, and 0.04 V for the pulse potential. Initial tests showed the independence between the calibrations of each metal by using a full factorial design.

The analysis of 8 samples of Portuguese and Spanish wines by ETAAS indicated that only copper levels were detected and quantified, obtaining  $Cu^{2+}$  concentrations varying between 0.011 and 0.535 mg/L. Considering the trace levels of heavy metals present in the wine samples, the ASDPV technique was selected, having obtained better results with the 4 min deposition step for standard calibration solution and sample solutions, which demanded an assisted digestion with  $HNO_3$  and  $H_2O_2$ .

The copper levels obtained from the analysis of wines by ASDPV as a function of those obtained by ETAAS showed a linear relationship, with an acceptable correlation coefficient and with a slope of 0.91, which indicates that the concentrations obtained by voltammetry are 0.91 times lower than those obtained by ETAAS. The ASDPV showed higher sensibility toward the copper (slope of  $22 \mu A.L.mg^{-1}$ ), than cadmium (slope of  $14.2 \mu A.L.mg^{-1}$ ) and lead (slope of  $13.5 \mu A.L.mg^{-1}$ ).

As a final conclusion, the ASDPV technique allows to analyze simultaneously three heavy metals using a cheap lab-made graphite composite working electrode. Its analytical performance allows considering its application in the voltammetric analysis of wines. However, there is space for improvement by optimizing the experimental procedure of solutions preparations for ASDPV analysis which will be addressed in future work.

## REFERENCES

- Aceto M, Abollino O, Bruzzoniti MC, Mentasti E, Sarzanini O, Malandrino M, Determination of metals in wine with atomic spectroscopy: flame-AAS, GF-AAS and ICP-AES, *Food Additives and Contaminants*, 2002, 19(2):126–133.
- Aceto M, Metals in wine, *Reviews in food and nutrition toxicity*, CRC Press, 2003, 169–203.
- Ambel MPC, Desarrollo de técnicas electroanalíticas aplicables a metales en fluidos biológicos de interés biosanitario: determinación de Cu en LCR (líquido cefalorraquídeo), PhD in Analytical Chemistry and Electrochemistry, Universidad de Cadiz, Spain, 1999, 200-220.
- Amerine MA, Berg HW, Cruess WV, *The technology of wine making*, 1972.
- Angelova VR, Ivanov AS, Braikov DM, Heavy metals (Pb, Cu, Zn and Cd) in the system soil-grapevine-grape, *Journal of the Science of Food and Agriculture*, 1999, 79:713–721.
- Antunovic V, Tripkovic T, Tomašević B, Baošić R, Jelic D, Lolic A, Voltammetric determination of lead and copper in wine by modified glassy carbon electrode, *Analytical Sciences*, 2021, 37(2):353-358.
- Barril C, Clark AC, Scollary GR, Chemistry of ascorbic acid and sulfur dioxide as an antioxidant system relevant to white wine, *Analytica Chimica*, 2012, 732:186–193.
- Berthon G, Aluminium speciation in relation to aluminium bioavailability, metabolism and toxicity, *Coordination Chemistry Reviews*, 2002, 228:319–341.
- Bertrand MJ, *Handbook of instrumental techniques for analytical chemistry*, 1997, 6633-6633.
- Bontidean I, Berggren C, Johansson G, Csöregi E, Mattiasson B, Lloyd JR, Jakeman KJ, Brown NL, Detection of heavy metal ions at femtomolar levels using protein-based biosensors, *Analytica Chimica*, 1998, 70:4162–4169.
- Bora FD, Bunea CL, Rusu T, Pop N, Vertical distribution and analysis of micro-, macroelements and heavy metals in the system soil-grapevine-wine in vineyard from North-West Romania, *Chemistry Central journal*, 2015, 9:2-10.
- Brainina KZ, Schafer H, Ivanova A, Khanina R, Determination of copper, lead and cadmium in whole blood by stripping voltammetry with the use of graphite electrodes, *Analytica Chimica Acta*, 1996, 330:175–181.
- Brainina KZ, Malakhova NA, Stojko NY, Stripping voltammetry in environmental and food analysis, *Fresenius' Journal of Analytical Chemistry*, 2000, 368:307–325.

- Brainina, KZ, Stozhko NY, Belysheva GM, Inzhevatova OV, Kolyadina LI, Cremisini C, Galletti M, Determination of heavy metals in wines by anodic stripping voltammetry with thick-film modified electrode, *Analytica Chimica Acta*, 2004, 514:227–234.
- Bruns R, Scarminio L, Neto BB, Statistical design - chemometrics, organic process research & development, 2006, 10:1082-1083.
- Cacho J, Castells JE, Esteban A, Laguna B, Sagristá N, Iron, copper, and manganese influence on wine oxidation, *American Journal of Enology and Viticulture*, 1995, 46:380–384.
- Castineira MM, Brandt R, Bohlen A, Jakubowski N, Development of a procedure for the multi-element determination of trace elements in wine by ICP-MS, *Fresenius Journal of Analytical Chemistry*, 2001, 370:553–558.
- Catarino S, Pimentel I, Curvelo-Garcia AS, Determination of copper in wine by ETAAS using conventional and fast thermal programs: validation of analytical method, *Journal of Analytical Atomic Spectrometry*, 2005, 26:73–78.
- Cesarino I, Cavaleiro ETG, Brett CMA, Characterization of graphite–polyurethane composite electrodes modified with organofunctionalized SBA-15 nanostructured silica in the presence of heavy metal ions. Application to anodic stripping voltammetry, *Microchimica Acta*, 2010, 171:1-9.
- Cornelis R, Caruso JA, Crews H, Heumann K, Handbook of elemental speciation: techniques and methodology, 2003, 25:429-441.
- Daniele S, Baldo MA, Ugo P, Mazzocchin GA, Determination of heavy metals in real samples by anodic stripping voltammetry with mercury microelectrodes: Part 1. Application to wine, *Analytica Chimica Acta*, 1989, 219:9–18.
- Danilewicz JC, Review of reaction mechanisms of oxygen and proposed intermediate reduction products in wine: central role of iron and copper, *American Journal of Enology and Viticulture*, 2003, 54:73-85.
- Danilewicz JC, Wallbridge, Further studies on the mechanism of interaction of polyphenols, oxygen, and sulfite in wine, *American Journal of Enology and Viticulture*, 2010, 61:166-175.
- Esparza I, Salinas I, Santamaría C, García-Mina JM, Fernández JM, Electrochemical and theoretical complexation studies for Zn and Cu with individual polyphenols, *Analytica Chimica Acta*, 2005, 543:267–274.
- Fei J, Peng Y, Tan H, Chen X, Yang J, Li J, Study on the electrochemical behavior and differential pulse voltammetric determination of rhein using a nanoparticle composite film-modified electrode, *Bioelectrochemistry*, 2007, 70:180-190.

- Freschi GPG, Dakuzaku CS, Moraes M, Nóbrega JA, Neto JAG, Simultaneous determination of cadmium and lead in wine by electrothermal atomic absorption spectrometry, *Spectrochimica Acta Part B: Atomic Spectroscopy*, 2001, 56:1987-1993.
- Galani-Nikolakaki S, Kallithrakas-Kontos N, Katsanos AA, Trace element analysis of Cretan wines and wine products, *Science of the Total Environment*, 2002, 285:155-163.
- Garrido J, Ayestarán B, Fraile P, Ancín C, Influence of pre-fermentation clarification on heavy metal lability in garnacha must and rosé wine using differential pulse anodic stripping voltammetry, *Journal of Agricultural and Food Chemistry*, 1997, 56:2843–2848.
- Ghoreishi SM, Behpour M, Khoobi A, Central composite rotatable design in the development of a new method for optimization, voltammetric determination and electrochemical behavior of betaxolol in the presence of acetaminophen based on a gold nanoparticle modified electrode, *Analytical Methods*, 2012, 4:2475-2485.
- González-Larraina M, González A, Médina B, Metallic ions for differentiation of red wines of the three regions of Denomination of Origin Rioja, *Connaissance de la Vigne et du Vin*, 1987, 21:127-140.
- Gunzler H, Williams A, Handbook of analytical techniques, Wiley-VCH, 2001, 2:1182-1200.
- Halicz L, Erel Y, Veron A, Pb isotope measurement by ICPMS; accuracy, precision and long time drift, *Journal of Analytical Atomic Spectrometry*, 1996, 17:186–189.
- Hanrahan G, Zhu J, Gibani S, Patil DG, Chemometrics: Experimental design, *Encyclopedia of Analytical Science*, 2005, 1:8–13.
- Helmerts E, Elements accompanying platinum emitted from automobile catalysts, *Chemosphere*, 1996, 33:405–419.
- Hernandez OLE, Naturaleza de sus complejos con  $CdCl_2$  y  $HgCl_2$  y su utilización en sensores electroquímicos, PhD in Chemistry, Universidad de Cadiz, Spain, 2006.
- Ibanez JG, Carreon-Alvarez A, Barcena-Soto M, Casillas N, Metals in alcoholic beverages: A review of sources, effects, concentrations, removal, speciation, and analysis, *Journal of Food Composition and Analysis*, 2008, 21:672–683.
- Kment P, Mihajlovic M, Ettlér V, Sebek O, Strnad L, Rohlova L, Differentiation of Czech wines using multielement composition—A comparison with vineyard soil, *Food Chemistry*, 2005, 91:157–165.
- Kreitman GY, Cantu A, Waterhouse AL, Elias RJ, Effect of Metal Chelators on the oxidative stability of model wine, *Journal of Agricultural and Food Chemistry*, 2013, 63:9480-9487.

- Kristl J, Veber M, Slekovec M, The contents of Cu, Mn, Zn, Cd, Cr and Pb at different stages of the winemaking process, *Acta Chimica Slovenica*, 2003, 50:123–136.
- Kurbanoglu S, Uslu B, Ozkan SA, Carbon-based nanostructures for electrochemical analysis of oral medicines, *Nanostructures for Oral Medicine*, 2017, 13:885-938.
- Laurie VF, Zúñiga MC, Sánchez VC, Santos LS, Cañete A, Azar CO, Ugliano M, Eduardo A, Reactivity of 3-sulfanyl-1-hexanol and catechol-containing phenolics in vitro, *Food Chemistry*, 2012, 131:1510-1516.
- Lin H, Li M, Mihailovič D, Simultaneous determination of copper, lead, and cadmium ions at a MoS<sub>2</sub>-xix nanowires modified glassy carbon electrode using differential pulse anodic stripping voltammetry, *Electrochimica Acta*, 2015, 154:184-189.
- Lopez FF, Cabrera C, Lorenzo ML, Lopez MC, Aluminum levels in wine, beer and other alcoholic beverages consumed in Spain, *The Science of the Total Environment*, 1998, 220:1–9.
- Maciel VV, Souza MM, Silva LO, Dias D, Direct determination of Zn, Cd, Pb and Cu in wine by differential pulse anodic stripping voltammetry, *Beverages*, 2019, 5:3-6.
- Mikkelsen O, Schröder KH, Voltammetry using a dental amalgam electrode for heavy metal monitoring of wines and spirits, *Analytica Chimica Acta*, 2002, 458:249–256.
- Moghaddam AB, Ganjali MR, Dinarvand R, Norouzi P, Saboury AA, Moosavi-Movahedi AA, Electrochemical behavior of caffeic acid at single-walled carbon nanotube: graphite-based electrode, *Biophysical Chemistry*, 2007, 128:30-37.
- Montgomery DC, *Design and analysis of experiments*, John Wiley and Sons, 1997, 1:1–26.
- Myers RH, *Response surface methodology*, Allyn & Bacon, 1971, 130-135.
- Naughton DP, Petroczi A, Heavy metal ions in wines: meta-analysis of target hazard quotients reveal health risks, *Chemistry Central Journal*, 2008, 2:22-22.
- Niwa O, Electroanalytical chemistry with carbon film electrodes and micro and nano-structured carbon film-based electrodes, *Bulletin of the Chemical Society of Japan*, 2005, 78:555-571.
- Oehme M, Lund W, Determination of cadmium, lead and copper in wine by differential pulse anodic stripping voltammetry, *Analytical and Bioanalytical Chemistry*, 1979, 294:391–397.
- Otto M, *Chemometrics: statistics and computer application in analytical chemistry*, 3<sup>rd</sup> edition, 1999, 201-205.
- Pennington JAT, Jones JW, *Aluminum in health: a critical review*, Marcel Dekker, CRC Press, 1989.

- Pohl P, What do metals tell us about wine?, *Trends in Analytical Chemistry*, 2007, 26:941–949.
- Pyrzyńska K, Analytical methods for the determination of trace metals in wine, *Reviews in Analytical Chemistry*, 2004, 34:69–83.
- Pyrzynska K, Chemical speciation and fractionation of metals in wine, *Chemical Speciation & Bioavailability*, 2007, 19:1-8.
- Ramírez-García S, Alegret S, Céspedes F, Forster RJ, Carbon composite electrodes: surface and electrochemical properties, *The Royal Society of Chemistry*, 2002, 127:1512-1519.
- Ranganathan S, Kuo TC, McCreery RL, Facile preparation of active glassy carbon electrodes with activated carbon and organic solvents, *Analytical Chemistry*, 1999, 71:3574–3580.
- Rassaei L, Sillanpää M, Bonné MJ, Marken F, Carbon nanofiber–polystyrene composite electrodes for electroanalytical processes, *Electroanalysis*, 2007, 19:1461-1466.
- Ribereau-Gayon P, Glories Y, Maujean A, Dubourdieu D, *Handbook of enology, the chemistry of wine stabilization and treatments*, John Wiley & Sons, 2006, 2:450-450.
- Riganakos KA, Veltsistas PG, Comparative spectrophotometric determination of the total iron content in various white and red Greek wines, *Food Chemistry*, 2003, 82:637–643.
- Saturno J, Valera D, Carrero H, Fernández L, Electroanalytical detection of Pb, Cd and traces of Cr at micro/nano-structured bismuth film electrodes, *Sensors and Actuators B: Chemical*, 2011, 159:92-96.
- Sauvage L, Frank D, Starne J, Millikan MB, Trace metal studies of selected white wines: an alternative approach, *Analytica Chimica Acta*, 2002, 458:223–230.
- Silva JJ, Paim LL, Stradiotto NR, Simultaneous determination of iron and copper in ethanol fuel using Nafion/carbon nanotubes electrode, *Electroanalysis*, 2014, 26:1794–1800.
- Siraj K, Kite S, Analysis of copper, zinc and lead using atomic absorption spectrophotometer in ground water of Jimma town of Southwestern Ethiopia, *International Journal of Chemical and Analytical Science*, 2013, 4:201–204.
- Solfrizzi V, Colacicco MA, D'Introno A, Capurso C, Parigi AD, Capurso SA, Capurso FTA, Panza F, Macronutrients, aluminium from drinking water and foods, and other metals in cognitive decline and dementia, *Journal of Alzheimer's Disease*, 2006, 10:303–330.
- Stozhko NY, Kolyadina LI, Electrochemical sample preparation for the voltammetric determination of heavy-metal ions in wine, *Journal of Analytical Chemistry*, 2005, 60:901–907.

- Tariba B, Metals in wine—Impact on wine quality and health outcomes, *Biological Trace Element Research*, 2011, 144:143–156.
- Telisman S, Colak B, Pizent A, Jurasović J, Cvitković P, Reproductive toxicity of low-level lead exposure in men, *Environmental Research*, 2007, 105:256–266.
- Telisman S, Jurasović J, Pizent A, Cvitković P, Blood pressure in relation to biomarkers of lead, cadmium, copper, zinc, and selenium in men without occupational exposure to metals, *Environmental Research*, 2001, 84:57–68.
- Teofilo RF, Ferreira M, Quimiometria II: planilhas eletrônicas para cálculos de planejamentos experimentais um tutorial, *Química nova*, 2006, 29:338-350.
- Tromp A, Klerk CA, Effect of copper oxychloride on the fermentation of must and wine quality, *South African Journal for Enology and Viticulture*, 1988, 9:31–36.
- Ugliano M, Kwiatkowski M, Vidal S, Capone D, Siebert T, Dieval JB, Aagaard O, Waters EJ, Evolution of 3-mercaptohexanol, hydrogen sulfide, and methyl mercaptan during bottle storage of sauvignon blanc wines. effect of glutathione, copper, oxygen exposure, and closure-derived oxygen, *Journal of Agricultural and Food Chemistry*, 2011, 59:2564-2572.
- Viviers M, Smith M, Wilkes E, Smith P, Effects of five metals on the evolution of hydrogen sulfide, methanethiol, and dimethyl sulfide during anaerobic storage of chardonnay and shiraz wines, *Journal of Agricultural and Food Chemistry*, 2013, 61:12385-12396.
- Viviers M, Smith M, Wilkes E, Smith P, Johnson D, The role of trace metals in wine reduction, *Wine & Viticulture Journal*, 2014, 29:38-40.
- Voica C, Dehelean A, Pamula A, Method validation for determination of heavy metals in wine and slightly alcoholic beverages by ICP-MS, *Journal of Physics*, 2009, 182:3-3.
- Volpe MG, Cara FL, Volpe F, Mattia DA, Serino V, Petitto F, Zavalloni C, Limone F, Pellecchia R, Prisco DPP, Stasio MDI, Heavy metal uptake in the enological food chain, *Food Chemistry*, 2009, 117:553–560.
- Wang J, Bian C, Tong J, Sun J, Xia S, L-Aspartic Acid/L-Cysteine/Gold nanoparticle modified microelectrode for simultaneous detection of copper and lead, *Thin Solid Films*, 2012, 520:6658–6663.
- Weng S, Tan-Qing W, Huang YF, Xue LS, Cheng J, Jin S, Liu SH, Wu D, Chen G, Anion-binding-induced electrochemical signal transduction in ferrocenyylimidazolium: combined electrochemical experimental and theoretical investigation, *Molecules*, 2019, 24:238-238.

- WHO (World Health Organization), Cadmium. Environmental health criteria 134, Geneva, 1992.
- WHO (World Health Organization), Copper. Environmental health criteria 200, Geneva, 1998.
- WHO (World Health Organization), Lead. Environmental health criteria 3. Geneva., 1977.
- Wiese C, Schwedt G, Strategy for copper speciation in white wine by differential pulse anodic stripping voltammetry, potentiometry with an ion-selective electrode and kinetic photometric determination, *Journal of Analytical Chemistry*, 1997, 56:718–722.
- Yang N, Swain GM, Jiang X, Nanocarbon electrochemistry and electroanalysis: current status and future perspectives, *Electroanalysis*, 2016, 28:27-34.
- Zerbinati O, Balduzzi F, Dell'Oro V, Determination of lithium in wines by ion chromatography, *Journal of Chromatography A*, 2000, 881:645–650.
- Zhu J, Gan H, Wu J, Ju H, Molecular machine powered surface programmatic chain reaction for highly sensitive electrochemical detection of protein, *Analytical Chemistry*, 2018, 90:5503–5508.
- Zsolt A, Norbert S, Emőke KS, Pál M, Krisztina G, László B, Direct sample introduction of wines in graphite furnace atomic absorption spectrometry for the simultaneous determination of arsenic, cadmium, copper and lead content, *Talanta*, 2008, 76:627-634.